

# Electroabsorption (Stark Effect) Spectroscopy of Mono- and Biruthenium Charge-Transfer Complexes: Measurements of Changes in Dipole Moments and Other Electrooptic Properties

Dennis H. Oh, Mitsuru Sano,<sup>†</sup> and Steven G. Boxer\*

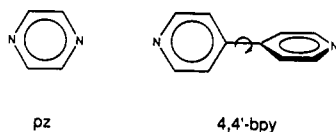
Contribution from the Department of Chemistry, Stanford University, Stanford, California 94305.

Received January 14, 1991

**Abstract:** Electroabsorption (Stark effect) spectra are reported for the charge-transfer transitions of  $(\text{NH}_3)_5\text{RuL}^{2+}$  and  $[(\text{NH}_3)_5\text{Ru}]_2\text{L}^{4+,5+}$ , where L is pyrazine (pz) or 4,4'-bipyridine (4,4'-bpy). The spectra permit experimental estimates of the susceptibility of the transition dipole moment to an electric field, the change in polarizability ( $\text{Tr}\Delta\alpha$ ), and the magnitude of the change in permanent electric dipole moment ( $|\Delta\mu|$ ) associated with many of the metal-to-ligand and metal-to-metal charge-transfer (MLCT and MMCT, respectively) transitions in these complexes. The observed electroabsorption spectra of the MLCT transitions of the monoruthenium complexes are interpreted as arising predominantly from  $\Delta\alpha$  and  $\Delta\mu$ . When L = pz and 4,4'-bpy, the observed values of  $|\Delta\mu|$  are  $(5.3 \pm 0.8)/f$  and  $(15.8 \pm 0.2)/f$  D, respectively, compared with the values of 16.5 and 27.1 D expected for full charge transfer from the metal to the geometric center of the ligand ( $f$  is a local electric field correction). Protonation of the monoruthenium complexes has relatively small effects on the observed  $\Delta\alpha$  and  $\Delta\mu$  when L = 4,4'-bpy, but when L = pz,  $\Delta\alpha$  appears to change its sign while  $\Delta\mu$  virtually disappears. A simple electrostatic model qualitatively accounts for the results and indicates that pyrazine allows a much greater degree of delocalization from the ruthenium than 4,4'-bipyridine whose pyridyl rings are probably not coplanar. The electroabsorption spectra of the MLCT region of the biruthenium complexes are very complicated and not quantitatively interpretable on the basis of current information, though interesting and qualitatively suggestive features appear. For the MMCT transitions in the biruthenium mixed-valence complexes where L is pz and 4,4'-bpy, the observed values of  $|\Delta\mu|$  are  $(0.7 \pm 0.1)/f$  and  $(28.5 \pm 1.5)/f$  D, respectively, compared with the values of 32.7 and 54.3 D expected for charge transfer in fully localized complexes. These latter results demonstrate that electronic delocalization between the two metals is essentially complete when the bridging ligand is pyrazine, whereas it is significant but incomplete when the bridge is 4,4'-bipyridine. In all complexes, the angle dependence of the electroabsorption demonstrates that  $\Delta\mu$  and the other field-interactive molecular properties are parallel to the transition dipole moment, as expected if the transition moment lies along the metal-ligand axis. The electroabsorption spectra of all of the monoruthenium and  $[(\text{NH}_3)_5\text{Ru}]_2\text{L}^{4+}$  complexes also show evidence for transitions that are weak or obscured in conventional absorption spectra; possible assignments are discussed within the context of a molecular orbital model.

## Introduction

Charge-transfer transitions are prominent features in the electronic absorption spectra of many transition-metal complexes such as  $(\text{NH}_3)_5\text{RuL}^{2+}$  and  $[(\text{NH}_3)_5\text{Ru}]_2\text{L}^{4+,5+}$ , where L is pyrazine (pz) or 4,4'-bipyridine (4,4'-bpy).<sup>1-3</sup> Because the metal-to-ligand



and metal-to-metal charge-transfer (MLCT and MMCT, respectively) transitions of these complexes nominally correspond to optically induced shifts of electronic charge density over relatively large distances, the initial and final states may have substantially different electrostatic properties, including electric dipole moments. Measurements of changes in such properties accompanying charge transfer provide information which reflects the electronic structures of these molecules in solution, and which is useful in understanding the dynamic changes in solvation that occur following optical excitation.<sup>4,5</sup> The potential technological applications of these compounds as molecular electronic devices have also generated interest and will largely depend on understanding as well as manipulating their electrostatic properties.<sup>6,7</sup> Yet, measurements of these important properties in transition-metal complexes have been rare and limited to studies of the solvent dependence of the charge-transfer band maxima.<sup>4,8</sup>

Electroabsorption, often called Stark effect spectroscopy, is the effect of an externally applied electric field on the molar absorption coefficient of a sample and provides a useful approach to study optical charge-transfer transitions of molecules.<sup>9</sup> The theoretical treatments developed for interpreting the electroabsorption of molecules in solution<sup>10,11</sup> have been successfully applied to nu-

merous experimental systems<sup>10,12-15</sup> including some inorganic charge-transfer spectra.<sup>16,17</sup> In many of these cases, the technique has yielded quantitative measures of the changes in permanent electric dipole moment ( $\Delta\mu$ ) and polarizability ( $\text{Tr}\Delta\alpha$ ) between two states involved in an optical transition, as well as the sus-

- (1) Ford, P.; Rudd, D. F. P.; Gaunders, R.; Taube, H. *J. Am. Chem. Soc.* **1968**, *90*, 1187-1194.
- (2) (a) Creutz, C.; Taube, H. *J. Am. Chem. Soc.* **1969**, *91*, 3988-3989. (b) Creutz, C.; Taube, H. *J. Am. Chem. Soc.* **1973**, *95*, 1086-1094. (c) Tom, G. M.; Creutz, C.; Taube, H. *J. Am. Chem. Soc.* **1974**, *96*, 7827-7830.
- (3) Sutton, J. E.; Sutton, P. M.; Taube, H. *Inorg. Chem.* **1979**, *18*, 1017-1021.
- (4) Winkler, J. R.; Netzel, T. L.; Creutz, C.; Sutin, N. *J. Am. Chem. Soc.* **1987**, *109*, 2381-2392.
- (5) Kozik, M.; Sutin, N.; Winkler, J. R. *Coord. Chem. Rev.* **1990**, *97*, 23-34.
- (6) (a) Launay, J. P. In *Molecular Electronic Devices II*; Carter, F. L., Ed.; Marcel Dekker, Inc.: New York, 1987; pp 39-54. (b) Launay, J. P.; Joachim, C. *J. Chim. Phys. Phys.-Chim. Biol.* **1988**, *85*, 1135-38. (c) Woitellier, S.; Launay, J. P.; Joachim, C. *Chem. Phys.* **1989**, *131*, 481-488.
- (7) *Supramolecular Photochemistry*; Balzani, V., Ed.; D. Reidel Publishing Co.: Dordrecht, 1987.
- (8) Creutz, C.; Chou, M. H. *Inorg. Chem.* **1987**, *26*, 2995-3000.
- (9) This paper describes changes in absorption due solely to the interaction of the externally applied electric field with the electronic states of the sample. This phenomenon has also been described by using the term electrochromism. Regrettably, that term has also been used to describe color changes that occur due to the injection of electrons from electrodes into lattice sites within a material [Coulton, R. J.; Guzman, A. M.; Rabalais, J. W. *Acc. Chem. Res.* **1978**, *11*, 170-176].
- (10) (a) Liptay, W., In *Excited States*; Lim, E. C., Ed.; Academic Press: New York, 1974, pp 129-229. (b) Liptay, W. *Ber. Bunsen-Ges. Phys. Chem.* **1976**, *80*, 207-217. (c) Liptay, W. *Z. Naturforsch.* **1965**, *20A*, 272-289. (d) Liptay, W. *Z. Naturforsch.* **1968**, *23A*, 1601-1612.
- (11) Lin, S. H. *J. Chem. Phys.* **1975**, *62*, 4500-4524.
- (12) Liptay, W.; Wortmann, R.; Schaffrin, H.; Burkhard, O.; Retinger, W.; Detzer, N. *Chem. Phys.* **1988**, *120*, 429-438.
- (13) Mathies, R. A. Ph.D. Thesis, Cornell University, 1974.
- (14) Ponder, M.; Mathies, R. J. *Phys. Chem.* **1983**, *87*, 5090-5098.
- (15) Lockhart, D. J.; Boxer, S. G. *Biochemistry* **1987**, *26*, 664-668, 2958.
- (16) (a) Davidsson, A.; Nordén, B. *Spectrosc. Lett.* **1977**, *10*, 447-454. (b) Davidsson, A. *Chem. Phys.* **1980**, *45*, 409-414. (c) Davidsson, A. *Chem. Phys. Lett.* **1983**, *101*, 65-68.
- (17) Oh, D. H.; Boxer, S. G. *J. Am. Chem. Soc.* **1989**, *111*, 1130-1131.

<sup>†</sup> Present address: Department of Chemistry, College of General Education, Nagoya University, Nagoya 464-01 Japan.

ceptibility of the transition dipole moment to an electric field. Such experiments provide an experimental approach for assigning charge-transfer bands and quantifying the degree of electronic delocalization in a molecular complex, thereby characterizing its electronic structure. Electric fields may also enhance obscured or inherently weak transitions, and possibly create new transitions that further elucidate the electronic structure of a molecule and suggest ways of manipulating it. Since useful nonlinear optical properties may arise in molecules when  $\Delta\mu$  is large,<sup>18</sup> electroabsorptive measurements should be of further interest and value in characterizing and exploiting these compounds.

In preliminary communications, we briefly reported an electroabsorption study of the MLCT absorption spectra of Ru(dimine)<sub>3</sub><sup>2+</sup> complexes,<sup>17</sup> as well as the first electroabsorption measurements of the MMCT transitions of biruthenium mixed valence complexes bridged by pyrazine and 4,4'-bipyridine.<sup>19</sup> In this paper, we discuss these latter results more fully, and extend the measurements and analysis to MLCT and MMCT transitions of related mono- and biruthenium complexes, with an emphasis on the dipolar properties related to their optical charge transfer.

### Experimental Section

**Materials.** [(NH<sub>3</sub>)<sub>5</sub>(H<sub>2</sub>O)Ru]<sup>2+</sup>(PF<sub>6</sub><sup>-</sup>)<sub>2</sub>, [(NH<sub>3</sub>)<sub>5</sub>Ru(pz)]<sup>2+</sup>(ClO<sub>4</sub><sup>-</sup>)<sub>2</sub>, and [(NH<sub>3</sub>)<sub>5</sub>Ru]<sub>2</sub>pz<sup>4+,5+</sup>(tos<sup>-</sup>)<sub>4,5</sub> were prepared according to methods described in the literature.<sup>2b,3</sup>

[(NH<sub>3</sub>)<sub>5</sub>Ru(4,4'-bpy)]<sup>2+</sup>(PF<sub>6</sub><sup>-</sup>)<sub>2</sub>. [(NH<sub>3</sub>)<sub>5</sub>(H<sub>2</sub>O)Ru]<sup>2+</sup>(PF<sub>6</sub><sup>-</sup>)<sub>2</sub> was added to a 20-fold excess of 4,4'-bipyridine in 10 mL of acetone, and the solution was stirred in the dark. After 2 h, the brown solution was filtered and treated with CH<sub>2</sub>Cl<sub>2</sub>, which induced precipitation of the desired product. Purification was accomplished by dissolving the complex in a minimum of acetone, filtering, and reprecipitating with CH<sub>2</sub>Cl<sub>2</sub>. The purity was checked by SP-sephadex C-25 chromatography and <sup>1</sup>H NMR: <sup>1</sup>H NMR (18 C, D<sub>2</sub>O)  $\delta$  8.46 (2 H, d), 8.42 (2 H, d), 7.65 (2 H, d), 7.48 (2 H, d). Anal. Calcd for C<sub>10</sub>H<sub>23</sub>F<sub>12</sub>P<sub>2</sub>RuN<sub>7</sub>: C, 18.99; H, 3.67; N, 15.51. Found: C, 18.93; H, 3.73; N, 14.79.

[(NH<sub>3</sub>)<sub>5</sub>Ru]<sub>2</sub>(4,4'-bpy)<sup>4+</sup>(PF<sub>6</sub><sup>-</sup>)<sub>4</sub> was prepared according to the literature.<sup>20</sup> The bromide salt was obtained by the addition of LiBr/acetone to the acetone solution of the hexafluorophosphate salt. The purity was checked by SP-sephadex C-25 chromatography. The identity of the compound was confirmed by cyclic voltammetry, <sup>1</sup>H NMR, and the electronic absorption spectra.<sup>3,20</sup>

[(NH<sub>3</sub>)<sub>5</sub>Ru]<sub>2</sub>(4,4'-bpy)<sup>3+</sup>(Br<sup>-</sup>)<sub>5</sub> was generated by mixing equimolar amounts of [(NH<sub>3</sub>)<sub>5</sub>Ru]<sub>2</sub>(4,4'-bpy)<sup>4+</sup>(Br<sup>-</sup>)<sub>4</sub> and [(NH<sub>3</sub>)<sub>5</sub>Ru]<sub>2</sub>(4,4'-bpy)<sup>6+</sup>(Br<sup>-</sup>)<sub>6</sub>. [(NH<sub>3</sub>)<sub>5</sub>Ru]<sub>2</sub>(4,4'-bpy)<sup>6+</sup>(Br<sup>-</sup>)<sub>6</sub> was generated by adding 2 equiv of Ce(IV) to [(NH<sub>3</sub>)<sub>5</sub>Ru]<sub>2</sub>(4,4'-bpy)<sup>4+</sup>(Br<sup>-</sup>)<sub>4</sub>.

(NH<sub>3</sub>)<sub>5</sub>Ru(pz)H<sup>3+</sup> and (NH<sub>3</sub>)<sub>5</sub>Ru(4,4'-bpy)H<sup>3+</sup> were prepared by dissolving the unprotonated salts in glycerol/H<sub>2</sub>O with 0.1 M HCl.

**Sample Preparation.** Samples were prepared by dissolving complexes to concentrations of 5–15 mM in either 50% (v/v) glycerol/water or [d<sub>3</sub>]glycerol/D<sub>2</sub>O, depending on the spectral region studied. Deuterated glycerol was prepared by chemical exchange at the hydroxyl groups by repeatedly adding 2 mL of D<sub>2</sub>O (99.9 atom % D, Aldrich) to 1 mL of glycerol (Baker), and equilibrating and freezing-pumping-thawing the mixture.

A schematic view of the electroabsorption cell is shown in Figure 1. The cell was constructed from microscope slides (Corning) with Ni (Aldrich) evaporated on the surface to form semitransparent electrodes (75 Å thick, ~1-cm<sup>2</sup> area, 50% transmission). The slides were separated by 0.001 in. (25.4 μm) thick Kapton tape strips (Saunders) and mechanically held together with clips. The bare Ni electrode surface was not chemically inert to samples containing acid or Ru(III) and, in such cases, was protected by rapidly dropping 150 μL of a 1-g/9-mL poly(methyl methacrylate)/acetonitrile solution onto the electrode spinning at 6000 rpm for 90 s on a photoresist spinner (Headway Research Instruments). A 0.5 ± 0.1 μm thick insulating layer of PMM formed, as measured on a Sloan Dektak IIa thickness measuring system.

Samples were prepared just before use, loaded into the electroabsorption cell, and immediately immersed in liquid nitrogen to minimize photosubstitution reactions.<sup>4,21</sup> Glasses of excellent optical quality resulted that depolarized visible and near-infrared light less than 10<sup>-4</sup>. The stability of the complexes at 77 K over the course of an experiment was checked by ensuring that the room temperature absorption spectra of the

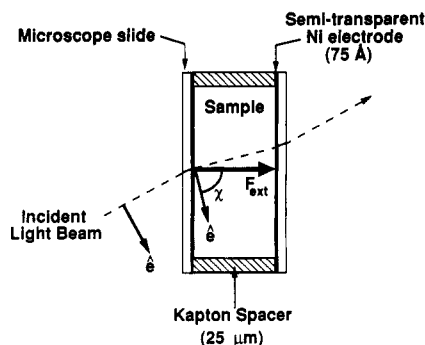


**Figure 1.** Schematic view of the electroabsorption cell.  $\hat{e}$  is the electric vector of the probe light,  $F_{\text{ext}}$  is the externally applied electric field, and  $\chi$  is the angle between  $\hat{e}$  and  $F_{\text{ext}}$ .

experimental samples conformed to those in the literature both before and after the experiment.

**Apparatus.** The technique and the apparatus used to measure the electroabsorption spectra have been essentially described.<sup>13,15</sup> The following modifications have been made: Electrical connections to the Ni electrodes of the sample were made by mechanical contact with alligator clips attached to the leads of a locally designed 0–4000 VAC source oscillating at 300–400 Hz. The light from a 100-W tungsten-halogen lamp (FDT, Sylvania) passed through a single monochromator (Spex Minimate) before probing the sample. The resolution of the monochromator was typically 1.8 nm and 4.75 nm in the regions 400–900 nm and 900–1800 nm, respectively. Two detectors were used over the spectral ranges studied: an RCA C30956E Si avalanche photodiode (400–900 nm) and a Judson IR J16 Ge photodiode (850–1800 nm). The electric field modulated light intensity was detected with a lock-in amplifier (Stanford Research Systems SR530) at the second harmonic of the field modulation frequency.

Absorption and electroabsorption spectra were obtained on the same spectrophotometer. Absorption spectra were recorded against blank cells containing glycerol/water glasses at 77 K. Neither the plain glycerol/water glasses nor glasses with 300 mM sodium tosylate exhibited an observable electroabsorption between 400 and 1800 nm.

**Method of Analysis.** When applied across a sample of nonoriented and immobilized molecules, an external electric field ( $F_{\text{ext}}$ ) causes a change in absorption,  $\Delta A(\nu)$ , which can often be described as a linear combination of zeroth, first, and second derivatives of the absorption band.<sup>10,22</sup>

$$\Delta A(\nu) = \left\{ A_x \cdot A(\nu) + B_x \cdot \frac{\nu}{15h} \cdot \frac{d(A(\nu)/\nu)}{d\nu} + C_x \cdot \frac{\nu}{30h^2} \cdot \frac{d^2(A(\nu)/\nu)}{d\nu^2} \right\} \cdot F_{\text{int}}^2 \quad (1)$$

$$A_x = D/3 + (3 \cos^2 \chi - 1)E/30$$

$$B_x = 5F + (3 \cos^2 \chi - 1)G \quad C_x = 5H + (3 \cos^2 \chi - 1)I$$

$$D = S^{(1)} \quad E = [3S^{(2)} - 2S^{(1)}]$$

$$F = \frac{1}{2} \text{Tr}(\Delta\alpha) + \mathbf{R}^{(1)} \cdot \Delta\mu$$

$$G + H = \frac{3}{2} \mathbf{m} \cdot \Delta\alpha \cdot \mathbf{m} + \frac{3}{2} \mathbf{R}^{(2)} \cdot \Delta\mu$$

$$H = |\Delta\mu|^2 \quad H + I = 3(\mathbf{m} \cdot \Delta\mu)^2$$

$\chi$  specifies the experimental angle between the external electric field and the light polarization at frequency  $\nu$  (see Figure 1);  $h$  is Planck's constant. The scalars  $S^{(1)}$  and  $S^{(2)}$ , and the vectors  $\mathbf{R}^{(1)}$  and  $\mathbf{R}^{(2)}$ , are functions of the transition moment polarizability and hyperpolarizability tensors.<sup>23</sup>

(22) Equation 1 has been derived assuming that only the positions and not the shapes of vibronic bands change in the presence of a field.<sup>10,13</sup> If the molecular properties change as a function of nuclear coordinates, underlying vibronic components of the band shape will behave differently in an electric field, and the overall band shape will deviate from the behavior predicted by eq 1 [Wortmann, R.; Elich, K.; Liptay, W. *Chem. Phys.* **1988**, *124*, 395–409]. Reimers and Hush also examine such cases using a very general treatment of electric field effects.<sup>27</sup>

(23)  $S^{(1)} = (1/|M|^2) \sum (A_{ii}A_{jj} + 2M_iB_{jj})$ ;  $S^{(2)} = (1/|M|^2) \sum (A_{ij}^2 + A_{ji}A_{ii} + 2M_iB_{ij} + 2M_jB_{ji})$ ;  $\mathbf{R}^{(1)} = (2/|M|^2) \sum M_iA_{ij}$ ;  $\mathbf{R}^{(2)} = (2/|M|^2) \sum (M_iA_{ji} + M_jA_{ij})$ .  $M$  is the transition moment, while  $A$  and  $B$  are the transition moment polarizability and hyperpolarizability tensors, respectively, which describe the response of the transition moment to an electric field;  $M(F) = M + A \cdot F + B \cdot B \cdot F$ . The subscripts  $i$  and  $j$  refer to the  $i$ th and  $j$ th molecular axes. These relationships and quantities are more explicitly defined elsewhere (see refs 10c, 10d, and 13).

(18) Oudar, J. L. *J. Chem. Phys.* **1977**, *67*, 446–457.

(19) Oh, D. H.; Boxer, S. G. *J. Am. Chem. Soc.* **1990**, *112*, 8161–8162.

(20) Tom, G. M. Ph.D. Dissertation, Stanford University, Stanford, CA, 1975.

(21) Durante, V. A.; Ford, P. C. *Inorg. Chem.* **1979**, *18*, 588–593.

**Table I.** Raw Results of Electroabsorption Measurements in 50% (v/v) Glycerol/H<sub>2</sub>O at 77 K

L	$d^a$ (Å)	$\nu_{\max}^b$ (cm <sup>-1</sup> )	$D \cdot f^2$ (10 <sup>-20</sup> m <sup>2</sup> /V <sup>2</sup> )	$E \cdot f^2$ (10 <sup>-20</sup> m <sup>2</sup> /V <sup>2</sup> )	$F \cdot f^2$ (10 <sup>-40</sup> C <sup>2</sup> m <sup>2</sup> /V)	$G \cdot f^2$ (10 <sup>-40</sup> C <sup>2</sup> m <sup>2</sup> /V)	$H \cdot f^2$ (10 <sup>-60</sup> C <sup>2</sup> m <sup>2</sup> )	$I \cdot f^2$ (10 <sup>-60</sup> C <sup>2</sup> m <sup>2</sup> )
(NH <sub>3</sub> ) <sub>3</sub> RuL <sup>2+</sup>								
pz	3.44 <sup>c</sup>	20 120	-1.3 ± 1.3	-8 ± 8	9 ± 7	15 ± 12	320 ± 100	670 ± 200
pzH <sup>+</sup>	3.39 <sup>d</sup>	18 800	0.15 ± 0.07	7 ± 6	-38 ± 6	-79 ± 7		
bpy	5.6 <sup>e</sup>	19 170	3.3 ± 0.8	26 ± 5	226 ± 10	420 ± 60	2760 ± 70	5040 ± 400
bpyH <sup>+</sup>	5.6 <sup>e</sup>	16 000	7 ± 4	34 ± 4	390 ± 100	770 ± 200	4300 ± 900	8400 ± 2000
[(NH <sub>3</sub> ) <sub>3</sub> RuLRu(NH <sub>3</sub> ) <sub>3</sub> ] <sup>5+</sup>								
pz	6.8 <sup>f</sup>	6250	-165 ± 40	-600 ± 200	8.6 ± 1.3	21.6 ± 1.0	5.6 ± 1.4	14.8 ± 1.0
bpy	11.3 <sup>g</sup>	8500	1 ± 7	-140 ± 190	2200 ± 1100	4300 ± 3000	9080 ± 900	16 400 ± 3000

<sup>a</sup> The distance between the ruthenium and the geometric center of the ligand, or between the two rutheniums. <sup>b</sup> Absorption maximum. <sup>c</sup> From ref 64. <sup>d</sup> Based on distance computed from the structure of (NH<sub>3</sub>)<sub>3</sub>Ru(pz)CH<sub>3</sub><sup>3+</sup>. See ref 65. <sup>e</sup> From ref 51. <sup>f</sup> From ref 53c.

$\Delta\alpha$  and  $\Delta\mu$  are the changes in the polarizability and permanent electric dipole moment, respectively, associated with an electronic transition between two states.<sup>24</sup>  $\mathbf{m}$  is a unit vector oriented along the transition dipole moment.  $\mathbf{F}_{\text{int}}$  is the internal electric field at the molecule, and depends on the externally applied field:  $\mathbf{F}_{\text{int}} = \mathbf{f} \cdot \mathbf{F}_{\text{ext}}$ , where  $\mathbf{f}$  is a tensor that depends on the dielectric constant of the medium and describes the local electric field correction.<sup>25</sup>

In principle, following corrections for multiple passes of light and path length changes with  $\chi$ ,<sup>14,15</sup> a successful decomposition of  $\Delta A(\nu)$  into its component derivatives with their  $\chi$  dependencies provides quantitative estimates of the molecular properties in eq 1 as well as their projections onto the transition dipole moment. The charge-transfer bands of the molecules considered here are generally so broad that direct numerical derivatives of the absorption spectra are noisy and unreliable. Alternatively, absorption spectra can be fit to sums of an arbitrary number of skewed Gaussian bands

$$A(\nu) = \sum_k A_k \exp[-(\nu - \nu_k)^2 / (\text{fwhm}_k)^2 - B_k(\nu - \nu_k)^3 - C_k(\nu - \nu_k)^4]$$

where  $A_k$  is the amplitude,  $\text{fwhm}_k$  is the full width at half-maximum of the pure Gaussian band,  $B_k$  and  $C_k$  are parameters determining the degree of skew and kurtosis, and  $\nu_k$  is the peak position of the  $k$ th Gaussian component in wavenumbers. The individual Gaussian bands do not necessarily have any physical significance; only the overall sum used as a fitting function to reliably model the band shape is important. A Marquardt nonlinear least-squares algorithm is used to optimize the fit to the absorption data and typically results in fits with residuals of less than 1%. Analytical differentiation of the fitting function then provides reliable zeroth, first, and second derivatives subsequently required to fit eq 1 to the  $\Delta A(\nu)$  spectra at  $\chi$  values of 90° and 54.7°. The fit yields values for  $A_k$ ,  $B_k$ , and  $C_k$  that then can be reduced to the quantities  $D \rightarrow I$  in eq 1.<sup>26</sup>

In general, much of our quantitative analysis relies on the simplest treatment of the data—we assume that successful fits of  $\Delta A(\nu)$  line shapes indicate that eq 1 is valid and that the molecular properties contained within it are constant throughout the  $\Delta A$  spectrum. Instances in which the  $\Delta A$  spectrum is not readily fit to eq 1 may arise if multiple electronic or vibronic transitions with differing field-interactive properties contribute to the overall absorption line shape.<sup>22,27,28</sup>

(24)  $\Delta\alpha = \alpha_f - \alpha_g$ ,  $\Delta\mu = \mu_f - \mu_g$ , where the subscripts  $g$  and  $e$  denote the initial (ground) and final (excited) states associated with the transition. In this paper,  $\Delta\alpha$  and  $\Delta\mu$  refer exclusively to quantities associated with absorptive transitions. For simplicity, we omit the previous notations of  $\Delta\alpha_A$  and  $\Delta\mu_A$  used to distinguish these quantities from those associated with emission (see refs 15, 17, and 19).

(25)  $f$  can be modeled in several ways [Böttcher, C. J. F. *Theory of Electric Polarization*, 2nd ed.; Elsevier: Amsterdam, 1973; Vol. 1, pp 74–86]. For example, when modeled by a spherical cavity surrounded by a medium whose dielectric constant,  $\epsilon$ , is between 2 and 4,  $f$  is 1.2–1.3. For an ellipsoidal cavity whose dimensions are appropriate for the molecules in this work and with  $\epsilon$  between 2 and 4,  $f$  is 1.0–1.2 along the long axis, and 1.2–1.5 along the short axis. For the more realistic case of a spherical or ellipsoidal dielectric embedded within another dielectric,  $f$  will approach the value of 1.0 even closer.  $\epsilon$  for glycerol/water glasses at 77 K used in this work has not been found in the literature, but is probably similar to the value of 3.5 measured for poly(vinyl alcohol) at 77 K [Lösche, M.; Fehér, G.; Okamura, M. Y. *Proc. Natl. Acad. Sci.* 1987, 84, 7537–7541]. Since the nature of  $f$  is uncertain and model-dependent, we report the molecular quantities of eq 1 in terms of  $f$  to distinguish true experimental errors from errors in modeling the local electric field. While  $f$  is not exactly known, it seems likely to be similar or the same for structurally and chemically homologous complexes in the same solvent and for similarly polarized transitions of the same molecule.

(26) This strategy succeeds since terms in eq 1 which depend on  $\chi$  vanish when  $\chi = 54.7^\circ$ , allowing calculation of terms that are independent of  $\chi$ .

The raw electroabsorptive quantities  $D \rightarrow I$  uniquely describe the response of a molecule's absorption to an external electric field. They depend only on the quality of the absorption and electroabsorption data, and the models used to fit them. They directly reflect the magnitudes and relative orientations of the fundamental molecular properties such as  $\Delta\alpha$  and  $\Delta\mu$  and may be useful when comparing one molecule to another, or one transition to another. While the terms  $D$ ,  $E$ ,  $H$ , and  $I$  readily yield  $S^{(1)}$ ,  $S^{(2)}$ ,  $|\Delta\mu|$ , and  $\mathbf{m} \cdot \Delta\mu$ , the terms  $F$  and  $G$  cannot be reduced further to  $\mathbf{R}^{(1)}$ ,  $\mathbf{R}^{(2)}$ ,  $\text{Tr}\Delta\alpha$ , and  $\mathbf{m} \cdot \Delta\alpha \cdot \mathbf{m}$  without the assumption that only  $\mathbf{R}^{(1)} \cdot \Delta\mu$  and  $\mathbf{R}^{(2)} \cdot \Delta\mu$ , or only  $\text{Tr}\Delta\alpha$  and  $\mathbf{m} \cdot \Delta\alpha \cdot \mathbf{m}$ , contribute to any first-derivative ( $B_k$ ) component (see eq 1). Even in cases that warrant this assumption, however,  $\mathbf{R}^{(1)}$  and  $\mathbf{R}^{(2)}$  cannot be obtained without independent information on the relative orientation and absolute sign of  $\Delta\mu$ . While  $\mathbf{R}^{(1)}$  and  $\mathbf{R}^{(2)}$  may well lie parallel to  $\Delta\mu$  in these particular complexes, we nevertheless tabulate the values of the products  $\mathbf{R}^{(1)} \cdot \Delta\mu$  and  $\mathbf{R}^{(2)} \cdot \Delta\mu$  that result when  $\text{Tr}\Delta\alpha$  and  $\mathbf{m} \cdot \Delta\alpha \cdot \mathbf{m}$  are assumed to be zero. In summary, we report the values of  $D \rightarrow I$  that are free of these assumptions but, where possible, we also reduce them to the fundamental field-interactive molecular properties, which are easier to discuss.

The reported errors in  $D \rightarrow I$  and in the reduced results are based on fits of eq 1 to multiple sets of measurements from at least two independently prepared replicate samples. These errors primarily reflect the experimental errors in precisely measuring both the external electric field (i.e., the sample thickness, which is accurate to 10%) and the absorption spectrum (which affects the contributions to the zeroth, first, and second derivatives to the fit of the  $\Delta A$  spectrum). The signal-to-noise ratio of the  $\Delta A$  spectra is not a principal source of variance in the results. The reported errors do not reflect variations that may result from differing interpretations of line shapes such as when multiple electronic or vibronic bands clearly overlap or when the molecular properties probed by the electric field strongly depend on the nuclear coordinates.<sup>22,27</sup>

## Results

Except where specifically noted, the representative electroabsorption spectra presented here were obtained at  $\chi = 90^\circ$ , and scaled to peak absorptions of unity and external electric fields of  $4 \times 10^7$  V/m to facilitate visual comparison. As predicted by eq 1, the observed  $\Delta A$  spectra scaled quadratically with applied field.

The regions spanned by the displayed fits in the figures of electroabsorption spectra represent the regions that were actually fit by eq 1. Tables I and II summarize the results of fits of eq 1 to the data in those cases where reasonable fits were possible. Table I presents the results in terms of the raw quantities  $D \rightarrow I$ . Table II presents the reduced results in terms of customarily used molecular, field-interactive quantities. Values for  $\mathbf{R}^{(1)}$ ,  $\mathbf{R}^{(2)}$ ,  $\text{Tr}\Delta\alpha$ , and  $\mathbf{m} \cdot \Delta\alpha \cdot \mathbf{m}$  are tabulated in each case with the assumption that only  $\mathbf{R}^{(1)} \cdot \Delta\mu$  and  $\mathbf{R}^{(2)} \cdot \Delta\mu$ , or only  $\text{Tr}\Delta\alpha$  and  $\mathbf{m} \cdot \Delta\alpha \cdot \mathbf{m}$  contribute to any first-derivative ( $B_k$ ) component (see eq 1).

**Monoruthenium Complexes.** The absorption and electroabsorption spectra in the MLCT region of (NH<sub>3</sub>)<sub>3</sub>Ru(pz)<sup>2+</sup> and (NH<sub>3</sub>)<sub>3</sub>Ru(4,4'-bpy)<sup>2+</sup> at 77 K are shown in Figure 2 along with fits of eq 1 to the electroabsorption spectra. The spectral regions fitted include weak electroabsorption features at energies below 17 000 cm<sup>-1</sup> that are not well fit by a sum of derivatives of the overall absorption; however, the presence of these low-energy features does not significantly affect the fit to the main MLCT

(27) Reimers, J. R.; Hush, N. S. In *Mixed-Valence Systems: Applications in Chemistry, Physics and Biology*; Praxides, K., Ed.; Kluwer Academic Publishers: Dordrecht, 1991; pp 29–50.

(28) Reimers and Hush, manuscript in preparation.

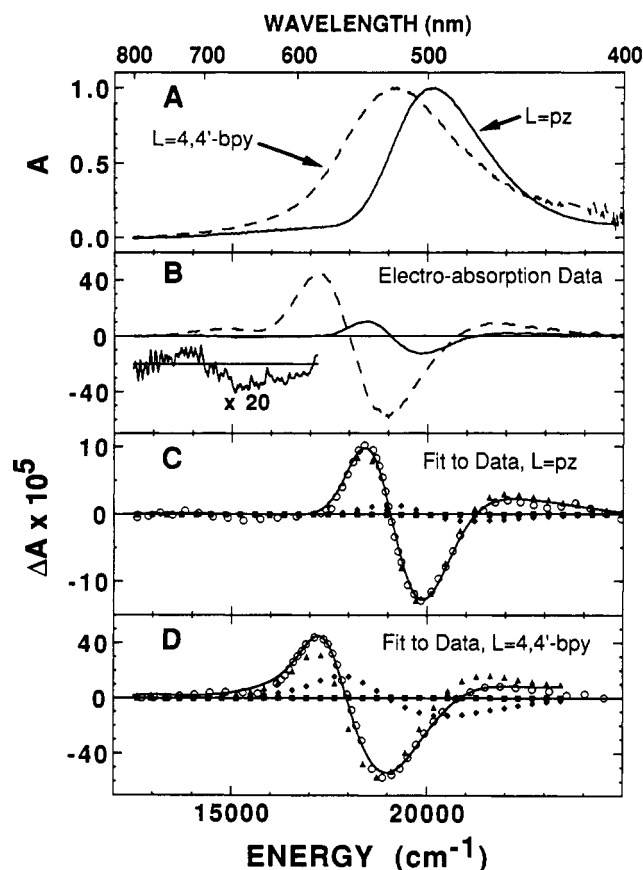


**Figure 2.** (A) Absorption and (B) electroabsorption spectra for  $(\text{NH}_3)_3\text{Ru}(\text{pz})^{2+}$  (—) and  $(\text{NH}_3)_3\text{Ru}(4,4'\text{-bpy})^{2+}$  (---) in 50% glycerol/ $\text{H}_2\text{O}$ , 77 K,  $F_{\text{ext}} = 4 \times 10^5 \text{ V/cm}$ ;  $\chi = 90^\circ$ . (C) Fit (—) to electroabsorption data (O) for  $L = \text{pz}$ ; note the expanded ordinate scale. (D) Fit (—) to electroabsorption data (O) for  $L = 4,4'\text{-bpy}$ . Zeroth (■), first (◆), and second (▲) derivative components of the fits are also shown. The inset in (B) displays data for  $L = \text{pz}$  magnified by 20 $\times$  in the region 12 500–17 000  $\text{cm}^{-1}$ .

band, and no attempt was made to deconvolute or exclude them in the fit.

A summary of the results follows: (1) Both complexes have  $\Delta A(\nu)$  line shapes that are almost exclusively dominated by the second derivative of the overall absorption and hence by  $\Delta\mu$ . When  $L = 4,4'\text{-bpy}$ , the observed  $|\Delta\mu|$  is about 3-fold larger than when  $L = \text{pz}$ . (2) In both cases, the relative contribution from the zeroth derivative is very small, indicating the transition moment polarizability and hyperpolarizability may be small enough to be neglected.<sup>29</sup> Hence, if  $R^{(1)}$  and  $R^{(2)}$  are also small enough to be neglected,  $\Delta\alpha$  appears to be substantially larger when  $L = 4,4'\text{-bpy}$  than when  $L = \text{pz}$ . (3) In both cases, the  $\chi$  dependencies of  $\Delta A(\nu)$  demonstrate that  $m \cdot \Delta\mu \approx |\Delta\mu|$ , and  $m \cdot \Delta\alpha \cdot m \approx \text{Tr} \Delta\alpha$  (see Table II); thus, the changes in dipole moments and polarizabilities lie parallel to the transition dipole moment, as one would expect for complexes with  $C_{2v}$  symmetry where MLCT occurs along the z-axis. (4) In both cases, a feature not associated with the main MLCT band appears in the  $\Delta A$  spectrum at low energy, and indicates the presence of another transition that is not obviously present in the conventional absorption spectrum, but is highly perturbable in an electric field. When  $L = \text{pz}$ , this feature is negative, while it is positive when  $L = 4,4'\text{-bpy}$ . These features

**Table II.** Reduced Results of Electroabsorption Measurements in 50% (v/v) Glycerol/ $\text{H}_2\text{O}$  at 77 K

L	$d^a$ (Å)	$\nu_{\text{max}}^b$ ( $\text{cm}^{-1}$ )	$S^{(1),f}$ ( $10^{-20} \text{ m}^2/\text{V}^2$ )	$S^{(2),f}$ ( $10^{-20} \text{ m}^2/\text{V}^2$ )	$R^{(1)}, \Delta\mu^f$ ( $10^{-40} \text{ C m}^2/\text{V}$ )	$R^{(2)}, \Delta\mu^f$ ( $10^{-40} \text{ C m}^2/\text{V}$ )	$\text{Tr}(\Delta\alpha)^f$ ( $10^{-40} \text{ C m}^2/\text{V}$ )	$m \cdot \Delta\alpha \cdot m^f$ ( $10^{-40} \text{ C m}^2/\text{V}$ )	$ \Delta\mu ^f$ ( $10^{-30} \text{ C m}$ )	$m \cdot \Delta\mu^f$ ( $10^{-30} \text{ C m}$ )	$ \Delta\mu _{\text{max}}^f$ ( $10^{-30} \text{ C m}$ )
pz	3.44 <sup>c</sup>	20120	-1.3 $\pm$ 1.3	-3 $\pm$ 4	9 $\pm$ 7	16 $\pm$ 12	18 $\pm$ 14 [16 $\pm$ 13] -76 $\pm$ 11	16 $\pm$ 13 [15 $\pm$ 12] -78 $\pm$ 8	18 $\pm$ 3 [5.3 $\pm$ 0.8]	18 $\pm$ 3 [5.4 $\pm$ 0.9]	55.0 [16.5] 54.4
pzH <sup>+</sup>	3.39 <sup>d</sup>	18800	0.15 $\pm$ 0.07	3 $\pm$ 2	-38 $\pm$ 6	-78 $\pm$ 8	-68 $\pm$ 10	-70 $\pm$ 8	52.6 $\pm$ 0.7 [15.8 $\pm$ 0.2]	51.0 $\pm$ 1.7 [15.3 $\pm$ 0.5]	90.4 <sup>e</sup> [27.1] 90.4 <sup>f</sup>
bpy	5.6 <sup>e</sup>	19170	3.3 $\pm$ 0.8	11 $\pm$ 2	226 $\pm$ 11	430 $\pm$ 50	450 $\pm$ 20 [410 $\pm$ 20]	430 $\pm$ 50 [390 $\pm$ 40] 800 $\pm$ 200	52.6 $\pm$ 0.7 [15.8 $\pm$ 0.2]	51.0 $\pm$ 1.7 [15.3 $\pm$ 0.5]	90.4 <sup>e</sup> [27.1] 90.4 <sup>f</sup>
bpyH <sup>+</sup>	5.6 <sup>e</sup>	16000	7 $\pm$ 4	16 $\pm$ 4	390 $\pm$ 100	800 $\pm$ 200	800 $\pm$ 200 [700 $\pm$ 170]	800 $\pm$ 200 [700 $\pm$ 200]	65 $\pm$ 7 [20 $\pm$ 2]	65 $\pm$ 7 [20 $\pm$ 2]	90.4 <sup>e</sup> [27.1] 90.4 <sup>f</sup>
pz	6.8 <sup>f</sup>	6250	-165 $\pm$ 40	-310 $\pm$ 90	8.6 $\pm$ 1.3	20.1 $\pm$ 0.2	17 $\pm$ 3 [16 $\pm$ 2]	20.1 $\pm$ 0.2 [18.1 $\pm$ 0.2]	2.4 $\pm$ 0.3 [0.7 $\pm$ 0.1]	2.60 $\pm$ 0.03 [0.8 $\pm$ 0.1]	109.1 [32.7] 181.1
bpy	11.3 <sup>g</sup>	8500	1 $\pm$ 7	-50 $\pm$ 60	2200 $\pm$ 1100	4000 $\pm$ 3000	4000 $\pm$ 2000 [4000 $\pm$ 2000]	4000 $\pm$ 3000 [4000 $\pm$ 3000]	95 $\pm$ 5 [28.5 $\pm$ 1.5]	92 $\pm$ 4 [27.6 $\pm$ 1.2]	181.1 [54.3] 181.1

<sup>a</sup> The distance between the ruthenium and the geometric center of the ligand, or between the two rutheniums. <sup>b</sup> Absorption maximum. <sup>c</sup> From ref 64. <sup>d</sup> Based on distance computed from the structure of  $(\text{NH}_3)_3\text{Ru}(\text{pz})\text{CH}_3^{3+}$ . See ref 51. <sup>e</sup> From ref 53c. <sup>f</sup> These values are limits which assume that only terms containing  $R^{(1)}$  and  $R^{(2)}$  contribute to the first derivative effect. See text. <sup>g</sup> These values are limits which assume that only terms containing  $\text{Tr}(\Delta\alpha)$  or  $m \cdot \Delta\alpha \cdot m$  contribute to the first-derivative effect. See text. <sup>h</sup>  $|\Delta\mu|_{\text{max}}$  is the value of  $|\Delta\mu|$  expected if a full electronic charge transfers across the distance,  $d$ . <sup>i</sup> If charge transfer to the proximal pyridyl moiety of 4,4'-bpy defines full charge transfer, then  $d = 3.57 \text{ Å}$  (ref 40), and  $|\Delta\mu|_{\text{max}} = 17.1 \text{ D}$  ( $5.70 \times 10^{-29} \text{ C m}$ ).

(29) Because the zeroth-derivative contribution reflects a sum of terms containing the transition moment polarizability and terms containing the transition moment hyperpolarizability (see eq 1 and footnote 23), a small zeroth derivative may have two interpretations: It may mean that the transition moment polarizability and hyperpolarizability are both negligibly small or, alternatively, that both are significant and nearly equal in magnitude but opposite in sign, thus canceling each other's effects. For now, in the absence of firm evidence supporting the very special, latter case, we adopt the former interpretation in presenting and discussing the results.

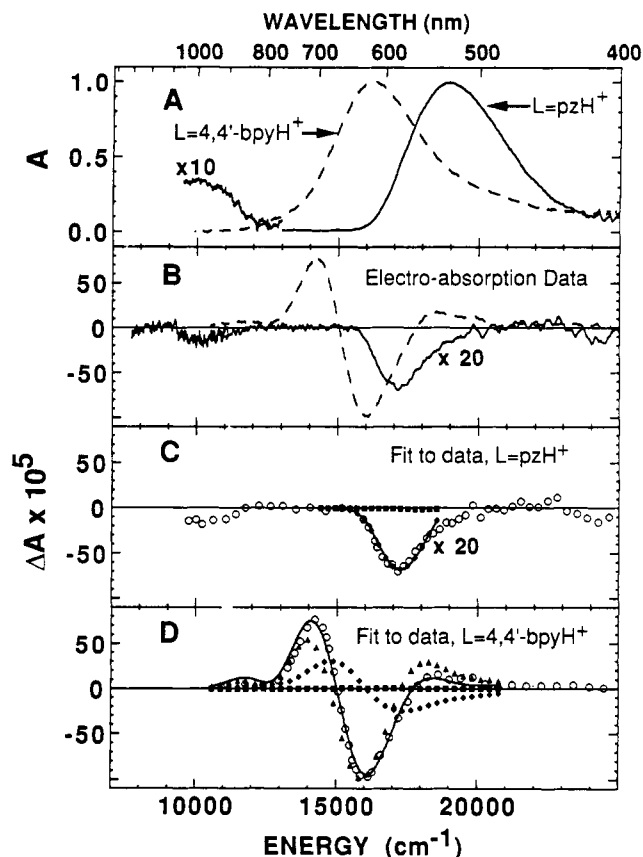


**Figure 3.** (A) Absorption and (B) electroabsorption spectra for  $(\text{NH}_3)_5\text{Ru}(\text{pz})\text{H}^{3+}$  (—) and  $(\text{NH}_3)_5\text{Ru}(4,4'\text{-bpy})\text{H}^{3+}$  (---) in 50% glycerol/ $\text{H}_2\text{O}$ , 77 K,  $F_{\text{ext}} = 4 \times 10^5$  V/cm;  $\chi = 90^\circ$ . (C) Fit (—) to electroabsorption data (O) for  $L = \text{pzH}^+$ . (D) Fit (—) to electroabsorption data (O) for  $L = 4,4'\text{-bpyH}^+$ . Zeroth (■), first (◆), and second (▲) derivative components of the fits are also shown. The absorption spectrum of  $(\text{NH}_3)_5\text{Ru}(\text{pz})\text{H}^{3+}$  has been magnified 10X below 13000  $\text{cm}^{-1}$ . The electroabsorption spectrum of  $(\text{NH}_3)_5\text{Ru}(\text{pz})\text{H}^{3+}$  and its fits have been magnified by 20X.

probably represent different portions of similar line shapes that are partially obscured by the electroabsorption of the main MLCT band. (5) With the exception of these low-energy features, the electroabsorption spectra are not further resolved into other transitions, either by the presence of additional features significantly deviating from a sum of derivatives of the overall absorption, or by a change in the  $\Delta A(\nu)$  line shape with  $\chi$ .

The effects of protonating these monoruthenium complexes are shown in Figure 3. Several observations are important: (1) As observed in the aqueous room temperature absorption spectra,<sup>1,30</sup> protonation in glycerol/ $\text{H}_2\text{O}$  glasses at 77 K shifts the MLCT band maxima to lower energies. When  $L = \text{pzH}^+$ , the maximum occurs at  $\sim 1300$   $\text{cm}^{-1}$  lower than in the unprotonated complex; when  $L = 4,4'\text{-bpyH}^+$ , it occurs  $\sim 3000$   $\text{cm}^{-1}$  to lower energy. Increases in the molar absorptivity also occur in both complexes when protonated (data not shown).<sup>1,30</sup> (2) In contrast to the  $\Delta A(\nu)$  spectra of the unprotonated complexes, the protonated pyrazine and bipyridyl complexes behave very differently from each other in an electric field. When  $L = \text{pzH}^+$ , little evidence exists for a  $C_x$  (second derivative) term in its  $\Delta A(\nu)$  spectrum; hence,  $\Delta\mu$  is very small.<sup>31</sup> When  $L = 4,4'\text{-bpyH}^+$ , the  $\Delta\mu$  contribution dominates the  $\Delta A(\nu)$  line shape, which is essentially identical with the unprotonated complex (cf. Figure 2B); the  $|\Delta\mu|$  of 20/fD is slightly larger than in the unprotonated form. (3) For  $L = \text{pzH}^+$ , the very small feature observed at  $\sim 17200$   $\text{cm}^{-1}$  of  $\Delta A(\nu)$  does fit well to the negative lobe of the inverted first derivative of the

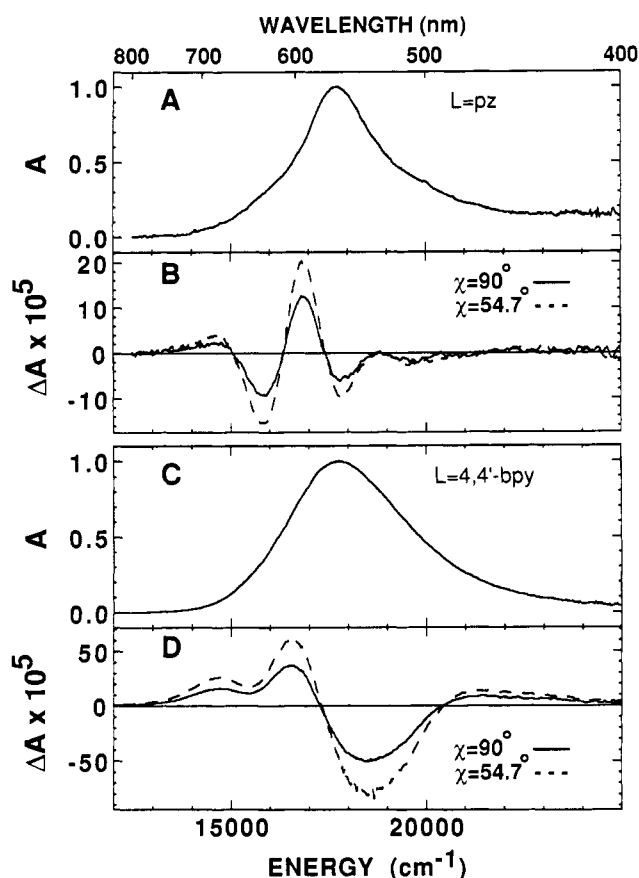


**Figure 4.** (A) Absorption and (B) electroabsorption spectra of  $[(\text{NH}_3)_5\text{Ru}]_2\text{pz}^{4+}$ . (C) Absorption and (D) electroabsorption spectra of  $[(\text{NH}_3)_5\text{Ru}]_2(4,4'\text{-bpy})^{4+}$ . Electroabsorption data at  $\chi = 90^\circ$  (—) and  $\chi = 54.7^\circ$  (---) are shown. 50% glycerol/ $\text{H}_2\text{O}$ , 77 K,  $F_{\text{ext}} = 4 \times 10^5$  V/cm.

overall absorption (a nearly pure  $B_x$  contribution), which may be due to either field-induced changes to the transition moment, changes in the polarizability, or both. The very small magnitude of the zeroth-derivative contribution suggests, however, that the electroabsorptive effect may be predominantly due to the change in polarizability rather than changes in the transition moment.<sup>29</sup> Tables I and II summarize the quantitative analysis of  $(\text{NH}_3)_5\text{Ru}(\text{pz})\text{H}^{3+}$  based on this particular interpretation. Alternatively, the feature may correspond to an  $A_x$  term or negative zeroth derivative corresponding to a weak low-energy absorption possessing a large susceptibility to an electric field. Since the overall  $\Delta A(\nu)$  can not be fit to a sum of derivatives of the overall absorption, either interpretation also suggests that the remainder of the  $\Delta A$  spectrum at higher energies ( $>19000$   $\text{cm}^{-1}$ ) is a convolution of at least two separate bands.<sup>68</sup> (4) Since the zeroth-derivative components in both electroabsorption spectra are essentially zero and do not change significantly from the unprotonated values, the data may provide good estimates for  $\text{Tr}\Delta\alpha$ .<sup>29</sup> Notably,  $\text{Tr}\Delta\alpha$  is negative when  $L = \text{pzH}^+$ , whereas it is positive when  $L = \text{pz}$ , 4,4'-bpy, and 4,4'-bpyH⁺. (5) As in the unprotonated forms, low-energy features that are very weak or obscured in the absorption spectra are enhanced in an electric field. When  $L = \text{pzH}^+$ , an isolated weak absorption occurs at  $\sim 10000$   $\text{cm}^{-1}$  with a corresponding feature in the electroabsorption spectrum centered at the same energy. Though the signal-to-noise ratio is far from optimal, the  $\Delta A$  spectrum in this region can be roughly fit to sums of derivatives of the overall absorption with a significant second-derivative contribution, suggesting a non-negligible  $\Delta\mu$  occurs with this transition.<sup>69</sup> When  $L = 4,4'\text{-bpyH}^+$ , a positive feature appears in the electroabsorption spectrum at  $\sim 12000$   $\text{cm}^{-1}$ . Its corresponding absorption is obscured by the main MLCT band.

**Biruthenium  $[(\text{NH}_3)_5\text{RuL}(\text{NH}_3)_5]^{4+}$  Complexes.** The visible absorption and electroabsorption spectra for  $[(\text{NH}_3)_5\text{Ru}]_2\text{L}^{4+}$  at

(30) Creutz, C. Ph.D. Thesis, Stanford University, 1970.

(31) When allowed to freely vary, the  $C_x$  term becomes negative, which carries no physical significance. Hence, the  $C_x$  weight was fixed at zero during the fit.

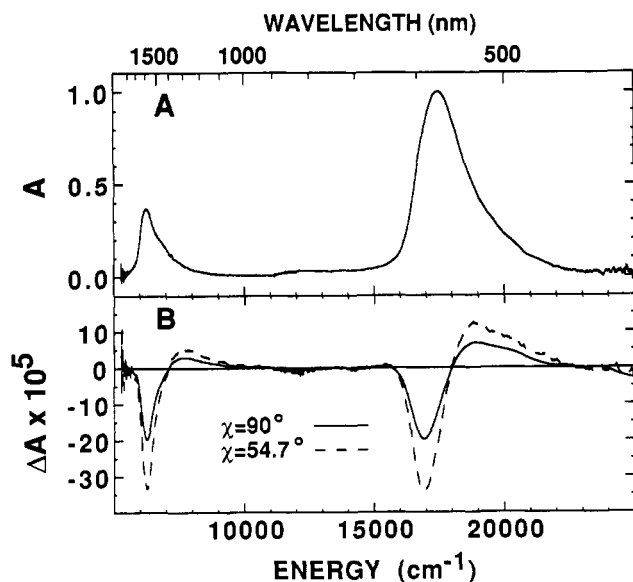


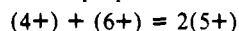
**Figure 5.** (A) Absorption and (B) electroabsorption spectra of  $[(\text{NH}_3)_5\text{Ru}]pz^{5+}$ . Electroabsorption data at  $\chi = 90^\circ$  (—) and  $\chi = 54.7^\circ$  (---) are shown. 50% glycerol/ $\text{H}_2\text{O}$ , 77 K,  $F_{\text{ext}} = 4 \times 10^5$  V/cm.

two different values of  $\chi$  are shown in Figure 4. The  $\Delta A$  is about 5-fold larger when  $L = 4,4'$ -bpy than when  $L = pz$ . From the overall line shape of both complexes, the  $\Delta A(\nu)$  spectra clearly indicate the presence of at least two bands, one roughly corresponding to the majority of the absorption, and the other corresponding to a very weak, lower energy transition that is unresolved in the absorption spectrum. The electroabsorptive effects from these multiple bands overlap and, unfortunately, are difficult to deconvolve uniquely without additional, independent information on the line shapes of the individual underlying absorption bands. The electroabsorption spectra at different values of  $\chi$  have the same line shape, however, indicating that the molecular properties of each underlying band probed by the electric field are identically oriented relative to their transition dipole moments. For both ligands, the ratio of  $\Delta A(54.7^\circ)/\Delta A(90^\circ)$  is  $\approx 1.67$ , which according to eq 1 indicates that if responsible for the electroabsorption,  $\Delta\mu$  and  $\Delta\alpha$  are oriented parallel to the transition dipole moment.

When  $L = pz$ , the electroabsorption under the peak of the observed absorption band (at energies  $>17000\text{ cm}^{-1}$ ) most resembles a first-derivative component since it possesses a zero crossing approximately at the same energy as the absorption maximum and does not have a positive feature at higher energy ( $>19000\text{ cm}^{-1}$ ). The negative feature centered at  $15800\text{ cm}^{-1}$  between two positive features qualitatively bears the signature of a second-derivative line shape due to a  $\Delta\mu$ ;  $\Delta A/A$  is approximately the same in this region as in the main MLCT band of  $(\text{NH}_3)_5\text{Ru}(pz)^{2+}$ . Thus, if  $\Delta\mu$  is principally responsible for the electroabsorption here, it may also be on the order of several Debyes.

When  $L = 4,4'$ -bpy, the electroabsorption line shape qualitatively resembles a second-derivative contribution centered at  $\sim 18500\text{ cm}^{-1}$  and is similar in magnitude to the monoruthenium complex, suggesting that the  $|\Delta\mu|$  associated with this band is similar to that in the monoruthenium complex. Unlike the case when  $L = pz$ , the low-energy positive feature at  $\sim 14500\text{ cm}^{-1}$  is not sufficiently resolved to unambiguously ascribe it to a particular derivative of an absorption band.

**Biruthenium  $[(\text{NH}_3)_5\text{RuLRu}(\text{NH}_3)_5]^{5+}$  Complexes.** The full absorption and electroabsorption spectra of  $[(\text{NH}_3)_5\text{RuLRu}(\text{NH}_3)_5]^{5+}$  from  $5500$  to  $25000\text{ cm}^{-1}$  are shown in Figures 5 and 6. They have been scaled to absorptions of unity in the visible (MLCT) bands. The MLCT spectra of the  $4,4'$ -bpy complex have been corrected for the comproportionation equilibrium



by using the comproportionation equilibrium constant,  $K_c = 20$ ,

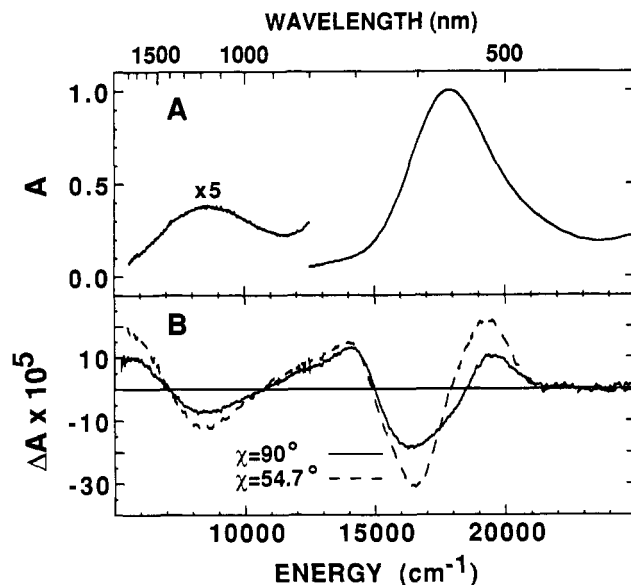


**Figure 6.** (A) Absorption and (B) electroabsorption spectra of  $[(\text{NH}_3)_5\text{Ru}]_2(4,4'\text{-bpy})^{5+}$ . Electroabsorption data at  $\chi = 90^\circ$  (—) and  $\chi = 54.7^\circ$  (---) are shown. 50% glycerol/ $\text{H}_2\text{O}$ , 77 K,  $F_{\text{ext}} = 4 \times 10^5$  V/cm. The near-infrared absorption ( $5500\text{--}12500\text{ cm}^{-1}$ ) has been magnified 5 $\times$ .

and assuming that the  $[(\text{NH}_3)_5\text{RuLRu}(\text{NH}_3)_5]^{6+}$  species does not contribute significantly to either absorption or electroabsorption spectra in this region.<sup>32</sup>

As in the  $[(\text{NH}_3)_5\text{Ru}]_2L^{4+}$  complexes, the visible absorption spectra for both mixed-valence complexes have complicated  $\Delta A(\nu)$  line shapes that are not well modeled by a linear combination of derivatives of the overall absorption band; thus, fits to the electroabsorption spectra in the visible region are not shown. The poor fits indicate the presence of multiple, unresolved transitions underlying the overall absorption, or the shortcomings of eq 1.<sup>22</sup> In an electric field, the bands do behave uniformly as a function of  $\chi$ , which indicates that the molecular properties which give rise to  $\Delta A$  are identically oriented with respect to the transition dipole moment throughout the overall absorption band. As with the  $[(\text{NH}_3)_5\text{Ru}]L^{4+}$  complexes,  $\Delta A(54.7^\circ)/\Delta A(90^\circ) \approx 1.67$  for the MLCT transitions of these complexes, specifying that these molecular properties are parallel to the transition moment.

Qualitatively, when  $L = pz$ , the  $\Delta A(\nu)$  spectrum in the visible region does not appear to have a large contribution from the second derivative or  $C_\chi$  term, while  $A_\chi$  and  $B_\chi$  terms contribute relatively more than in the monoruthenium complex. From a marginal fit to a sum of derivatives of the overall absorption,  $|\Delta\mu|$  is small and crudely estimated to be  $\sim 2.5/fD$ . When  $L = 4,4'$ -bpy, the visible  $\Delta A$  spectrum corrected for comproportionation has two positive features separated by one negative feature at  $\sim 16500\text{ cm}^{-1}$ , roughly resembling the second derivative of an absorption band that underlies the overall absorption. Qualitatively, this line shape indicates the presence of a MLCT transition in which  $\Delta\mu$  dominates over other properties. Spectra are displayed at two different values of  $\chi$  to give an idea of the magnitude of the effect's change with angle. While the positions of minima and maxima vary little with  $\chi$ , the zero crossings of the spectra do. We note, however, that the  $\chi = 90^\circ$  and  $\chi = 54.7^\circ$  spectra scale exactly with each other prior to correcting for comproportionation; thus, the difference in zero crossings is likely to be an artifact due to imperfect scalings during the comproportionation corrections.

The electroabsorption spectra of mixed-valence species in the near-infrared (MMCT) region show the most dramatic differences

(32) The value of  $K_c = 20$  was determined in aqueous solution at 298 K [Sutton, J. E.; Taube, H. *Inorg. Chem.* **1981**, *20*, 3125–3134]. We assume that this value is valid for glycerol/water solutions, and that the equilibrium concentrations of the various species at 298 K exist at 77 K when the sample is rapidly frozen to form a glass. Spectra of  $4+$  and  $5+$  complexes at similar concentrations were used for the comproportionation correction.

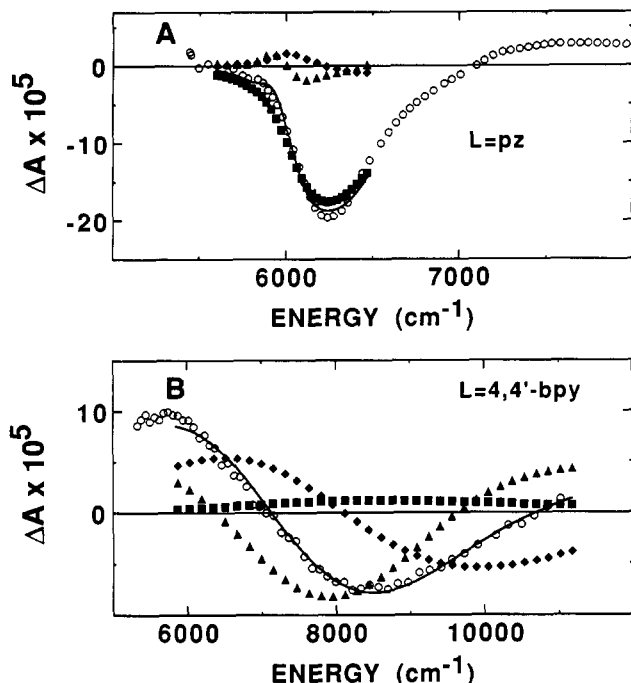


**Figure 7.** (A) Fit (—) to electroabsorption data (O) for  $[(\text{NH}_3)_3\text{Ru}]_2\text{pz}^{2+}$  at  $\chi = 90^\circ$  in the near-infrared region of the spectrum. Zeroth (■), first (◆), and second (▲) derivative components of the fits are also shown. (B) Fit (—) to electroabsorption data (O) for  $[(\text{NH}_3)_3\text{Ru}]_2(4,4'\text{-bpy})^{5+}$  at  $\chi = 90^\circ$  in the near-infrared region of the spectrum. Zeroth (■), first (◆), and second (▲) derivative components of the fits are also shown.

as a function of the bridging ligand. When  $L = \text{pz}$ , the largest electroabsorption occurs in the nominal intervalence charge-transfer band where the electric field appears to cause essentially a decrease in absorption at energies below  $6500\text{ cm}^{-1}$ , while at energies higher than  $7000\text{ cm}^{-1}$  the absorption increases in a complex fashion.<sup>33</sup> The entire  $\Delta A(\nu)$  spectrum does not satisfactorily reduce to a sum of derivatives of the overall absorption line shape. However, little evidence appears for a very significant first- or second-derivative contribution to the  $\Delta A(\nu)$  line shape, which is well modeled primarily by a negative zeroth-derivative ( $A_0$ ) term, especially at energies below  $6500\text{ cm}^{-1}$  (Figure 7A). Tables I and II present the analysis for energies below  $6500\text{ cm}^{-1}$ , which shows that while the terms responsible for the negative zeroth derivative are very large, the values of the terms responsible for the first derivative are similar to those of  $(\text{NH}_3)_3\text{Ru}(\text{pz})^{2+}$ . The values responsible for the second-derivative component are also very small indeed. The  $\Delta A$  spectrum also shows a weak effect at  $\sim 12000\text{ cm}^{-1}$ , which suggests the presence of a state of intermediate energy whose absorption is normally obscured by the wings of the stronger MMCT and MLCT bands.

When  $L = 4,4'$ -bipyridine, a linear combination of derivatives of the observed absorption band closely models the  $\Delta A(\nu)$  line shape of the near-infrared band (Figure 7B). The second-derivative component dominates the spectrum, though the zeroth and first derivatives also contribute, indicating that the transition moment and polarizability changes are nonnegligible. Unfortunately, the extremely short path lengths required for the electroabsorption samples combined with an inherently small extinction coefficient resulted in an intervalence absorption band of low optical density that was frequently skewed by small but relatively significant slopes in the base line. Such artifacts tend to propagate as zeroth- and first-derivative components and result in large errors in the calculated values of  $D$ ,  $E$ ,  $F$ , and  $G$  and their reduced quantities.

(33) A similar line shape exists in the electroabsorption of the complex in poly(vinyl alcohol) at both 77 and 298 K, with the exception of a slight blue shift of the  $\Delta A$  minimum relative to the absorption maximum (data not shown), suggesting that the electroabsorptive effect and the molecular properties responsible for it may be solvent dependent.

## Discussion

The molecules studied exhibit the full range of possible effects in an electric field. Our discussion of the electroabsorption results focuses primarily on the change in dipole moment,  $|\Delta\mu|$ , between the ground and excited state since this property is unambiguously extracted from the data by using eq 1 and intimately depends on the charge transfer that so uniquely distinguishes these complexes.

**Monoruthenium Complexes.** The mononuclear complexes possess electronic absorption spectra that feature intense bands assigned as metal-to-ligand charge-transfer transitions.<sup>1,34</sup> Consistent with this assignment, effects due to  $|\Delta\mu|$  dominate the electroabsorption of the visible absorption bands, demonstrating that the electronic distributions of the ground and excited states differ, sometimes substantially. Complementing this result, earlier work by Ford et al. determined that the  $pK_a$  of the pyrazine's free nitrogen in  $(\text{NH}_3)_3\text{Ru}(\text{pz})^{2+}$  is several units higher in the MLCT excited state than in the ground state, suggesting that the ligand's electron density is greater in the MLCT state.<sup>1</sup>

While the experimentally observed values of  $|\Delta\mu|$  qualitatively correlate with the distance between the metal and the ligand, they are quantitatively smaller than expected for the shift of a full electronic charge from the metal to the geometric center of the ligand (Table II). If a full electronic charge moves from the metal to the geometric center of the accepting ligand, then the maximum observable  $|\Delta\mu|$  is the product of a unit charge and the distance traveled, excluding effects due to the local electric field. Thus, when  $L = \text{pz}$ ,  $\Delta\mu_{\text{max}}$  is 16.5 D (Table II), and the observed  $|\Delta\mu|$  of  $5.2/f$  D permits a very crude estimate of 32/% of full charge transfer.<sup>35</sup> When  $L = 4,4'$ -bpy, a similar calculation concludes that 58/% of full charge transfer occurs; alternatively, if the distance from the ruthenium to the center of the proximal pyridyl ring is used to define full charge transfer, then 89/% charge transfer occurs. Since  $f$  must be greater than or equal to unity, these results indicate that less than full charge transfer occurs. If the differences in the  $|\Delta\mu|$  observed for these complexes are predominantly due to differences in electronic delocalization, they are consistent with earlier observations that the  $pK_a$  of the distal nitrogen of pyrazine complexed to ruthenium pentaammine is 2 units larger than in the free ligand, while that in bipyridine changes less.<sup>1,30</sup> These results all indicate that the extent of metal-ligand interactions (covalency) is much greater when the ligand is pyrazine than when it is 4,4'-bipyridine.

The differences between the observed and the maximum values of  $|\Delta\mu|$  have also been observed in  $\text{Ru}(\text{diimine})_3^{2+}$  complexes<sup>17</sup> and may have several origins. A reduction in apparent  $|\Delta\mu|$  by electrostatic interactions between the ammine or spectator ligand dipoles and the metal charge has been suggested by Reimers and Hush.<sup>27</sup> Surprisingly, this has been calculated to account for approximately half of the difference between the  $|\Delta\mu|_{\text{max}}$  and the observed  $|\Delta\mu| \cdot f$ . Of greater chemical interest, mixing between the metal and the ligand orbitals will result in electronic delocalization in the ground and/or the excited state and diminish their permanent electric dipole moments. Back-bonding to ligand  $\pi^*$  orbitals provides one mechanism for delocalizing the metal charge onto the pyrazine ligand and, in previous molecular orbital analyses, has been estimated to result in  $\sim 80\%$  of full optical charge transfer.<sup>8,34</sup> Augmented self-consistent field (ASCF) calculations arrive at a similar value of 0.12 of an electronic charge delocalizing as a result of  $\pi$ -back-bonding, accounting for about one-third of the difference between  $|\Delta\mu|_{\text{max}}$  and  $|\Delta\mu| \cdot f$ .<sup>27</sup> These treatments often assume that the metal and ligand interact to the same extent in the ground and MLCT states; however, differing extents of metal-ligand orbital mixing in ground and MLCT states

(34) Zwicker, A. M.; Creutz, C. *Inorg. Chem.* **1971**, *10*, 2395-2399.

(35) The results from the unprotonated pyrazine complex are similar in some respects to those obtained for 1-(dimethylamino)-2,6-dicyano-4-methylbenzene, a structurally analogous organic molecule with charge-transfer character.<sup>12</sup> The data for the  $L = \text{pz}$  case, when corrected for the local field by using  $f = 1.3$ , yields an observed  $|\Delta\mu|$  of 4 D, essentially the same as the value of 3.7 D observed for the benzene derivative. The experimentally observed changes in polarizability, however, are quite different in the two complexes.



could result in an even smaller  $|\Delta\mu|$ . For example, the existence of bonding interactions between the partially occupied metal  $d\pi$  and occupied ligand  $\pi$  orbitals have also been noted<sup>36</sup> and suggest an additional mechanism for electronic delocalization in the ground state. A previous discrepancy between the back-bonding stabilization energies obtained from spectral and electrochemical data led to the suggestion that  $\sigma$  orbital interactions may also be important mechanisms of delocalization that are not probed by the electronic transitions between  $\pi$  orbitals.<sup>34</sup> Finally, a solvent-solute or ion pair interaction that alters the nuclear or electronic structure cannot be excluded as a possibility.<sup>37,38</sup> When  $L = pz$ , the observed electroabsorption is approximately the same in both PVA and frozen glycerol/water (data not shown), suggesting that such interactions are not significant, though this possibility has not been systematically explored.

The electronic consequences of protonating the distal nitrogen of the heterocyclic ligand further illustrate the dramatic differences in the coupling between the ruthenium complexed to pyrazine and to 4,4'-bipyridine. Protonation removes any observable effect assignable to  $|\Delta\mu|$  corresponding to the major visible absorption of the pyrazine complex. The absence of shifts in the absorption spectrum of  $(NH_3)_5MpzCH_3^{3+}$  ( $M = Ru, Os$ ) with solvent polarity or with Gutmann donor number has been previously noted<sup>8,39</sup> and may be analogous to the electroabsorption result for  $(NH_3)_5Ru(pz)H^{3+}$ , which indicates that little charge redistribution occurs upon absorption of light. In both cases, the additional positive charge of the distal nitrogen may create an additional electrostatic capacity for delocalization through back-bonding interactions.<sup>30</sup> A previous spectral analysis<sup>39</sup> of  $(NH_3)_5Ru(pz)H^{3+}$  concluded that protonation decreases the energy difference between the metal  $d\pi$  and pyrazine  $\pi^*$  orbitals by 12 000  $cm^{-1}$ , making the metal and ligand orbitals nearly degenerate while increasing the metal-ligand coupling by 2600  $cm^{-1}$ . The interaction between the ruthenium and the pyrazine appears to be so strong that others have suggested that a  $Ru=N$  double bond is a more appropriate description.<sup>4</sup> This idea is consistent with the absence of an observable  $|\Delta\mu|$  in the electroabsorption.

In contrast, protonation does not decrease the observed  $|\Delta\mu|$  in the 4,4'-bipyridine complex; indeed,  $|\Delta\mu|$  actually increases slightly upon protonation. This result may indirectly reflect the conformation of the bipyridinium ligand. A planar bipyridinium conformation was once suggested to explain the dramatic decrease in the transition energy of the MLCT band relative to the unprotonated complex.<sup>30</sup> Arguing against such a model, however, a structural study of *N*-methyl-4,4'-bipyridinium cation ( $MQ^+$ ) in  $[(2,2'-bpy)Re(CO)_3(MQ^+)](PF_6)_2$  found that the two rings of  $MQ^+$  were not coplanar but rotated 47° from each other.<sup>40</sup> Moreover, theoretical efforts have predicted that the 4,4'-bipyridinium dication should be nonplanar, albeit essentially free to rotate, in solution at room temperature.<sup>41</sup> Since a planar conformation would allow greater electronic delocalization between the two pyridyl rings, and hence from the ruthenium as well, the large value of  $|\Delta\mu|$  observed in the electroabsorption experiment supports the following alternative model, which is based solely on simple classical electrostatic arguments. The principal effect of protonating  $(NH_3)_5Ru(4,4'-bpy)^{2+}$  in frozen solution may simply be to stabilize the MLCT state by a favorable Coulombic interaction of the positively charged proton with the excited electron density on the bipyridine rings, without directly altering the electronic coupling between the rings via their conformation or between the metal and the ligand. A destabilization of the ground state should likewise occur due to repulsive electrostatic interactions between the positive charges on the ruthenium and

the proton. A significantly lowered MLCT transition energy would result, but no decrease in  $\Delta\mu$  would occur. Conceivably, the positive charge of the protonated bipyridine ring may allow greater charge transfer to occur, resulting in a larger  $|\Delta\mu|$ , as observed. Whether the bipyridyl radical anion ligand would become planar if allowed to evolve in a fluid system is an interesting question that, while not immediately relevant to this discussion of the initially excited, Franck-Condon state, has been addressed at length elsewhere.<sup>4,42</sup>

The differences between  $L = pzH^+$  and  $L = 4,4'-bpyH^+$  complexes also extend to the estimates of  $Tr\Delta\alpha$ . When  $L = pzH^+$ , an unusual negative first-derivative component appears in the  $\Delta\Delta$  spectrum which, given our tentative assumptions,<sup>29</sup> suggests the polarizability in the excited state is smaller than in the ground state ( $\Delta\alpha < 0$ ). This phenomenon may be intimately related to the nature of the metal-ligand interactions. Because protonation appears to bring the metal  $d\pi$  and the ligand  $\pi^*$  orbitals into near degeneracy, the resultant molecular orbitals have been characterized as truly bonding and antibonding, rather than mostly metal or ligand, in character.<sup>4</sup> Such a model intuitively predicts greater electronic delocalization and polarizability in the ground state due to a formally conjugated  $\pi$  system extending from the ruthenium through the pyrazine. Upon excitation to the antibonding state, however, the metal-ligand  $\pi$  interaction is broken, diminishing conjugation and the polarizability in the excited state. On the other hand, MLCT in  $(NH_3)_5Ru(4,4'-bpyH^+)^{3+}$  is associated with a positive  $Tr\Delta\alpha$ . Since this complex does appear to be well described as having orbitals of largely either metal or ligand character,<sup>4</sup> charge transfer formally corresponds to moving an electron from the metal to the bipyridine, an essentially larger molecular moiety. Within this crude picture, where polarizability scales with molecular size, one might expect a larger polarizability in such a charge-transfer state.

All of the electroabsorption spectra also possess low-energy features that are prominent relative to the weak absorptions to which they correspond. Interestingly, a very similar phenomenon<sup>17</sup> occurs in the electroabsorption spectra of  $Ru(diimine)_3^{2+}$  in an absorption band that, in the case of  $Ru(bpy)_3^{2+}$ , has been assigned to a very weakly allowed singlet to triplet MLCT transition.<sup>43</sup> Alternatively, molecular orbital models predict that, in addition to the primary MLCT band, monoruthenium  $d^6$  metal complexes should also possess MLCT transitions at lower energies which are essentially from nonbonding metal  $d_\pi$  to ligand  $\pi^*$  orbitals.<sup>34,36</sup> Since they involve orbitals that do not overlap, such transitions should both possess greater charge-transfer character<sup>8</sup> and be extremely weak, perhaps gaining intensity through vibronic coupling. Additionally, these weak absorptions may have transition dipole moments that are enhanced to a greater degree than the strongly allowed transitions in an electric field, perhaps by mixing with other nearby MLCT states which are dipolar as well as highly allowed. In contrast to the electroabsorption spectra, the absorption spectra of such transitions are difficult to observe in these complexes except in a few instances where the transition is sufficiently lower in energy to be resolved from the intense main MLCT band.<sup>4,39</sup>

In the case where  $L = pz$ , a negative feature occurs at  $\sim 15\,500\,cm^{-1}$ . If the effect is principally the same as in the main MLCT band (i.e., a second derivative) or is a zeroth derivative, then the low-energy transition occurs at  $\sim 15\,500\,cm^{-1}$ . By using the molecular orbital model introduced by Zwickel and Creutz,<sup>34</sup> this observation, along with the peak maximum of the main MLCT band at 20 120  $cm^{-1}$ , allows an estimate of the energy of stabilization ( $E_s$ ) due to the metal-ligand interaction as being  $\sim 4600$

(36) Lauher, J. W. *Inorg. Chim. Acta* **1980**, *39*, 119-123.

(37) Curtis, J. C.; Sullivan, B. P.; Meyer, T. J. *Inorg. Chem.* **1983**, *22*, 224-236.

(38) Begum, M. K.; Grunwald, E. J. *Am. Chem. Soc.* **1990**, *112*, 5104-5110.

(39) Magnuson, R. H.; Taube, H. J. *Am. Chem. Soc.* **1975**, *97*, 5129-5136.

(40) Chen, P.; Curry, M.; Meyer, T. J. *Inorg. Chem.* **1989**, *28*, 2271-2280 and references therein.

(41) von Nagy-Felsobuki, E. I. *J. Heterocycl. Chem.* **1988**, *25*, 33-37.

(42) (a) Chen, P.; Danielson, E.; Meyer, T. J. *J. Phys. Chem.* **1988**, *92*, 3708-3711. (b) Lee, P. C.; Schmidt, K.; Gordon, S.; Meisel, D. *Chem. Phys. Lett.* **1981**, *81*, 242. (c) Schanze, K. S.; Neyhart, G. A.; Meyer, T. J. *J. Phys. Chem.* **1986**, *90*, 2182-2193. (d) Reimers, J. R.; Hush, N. S. *Inorg. Chem.* **1990**, *29*, 2686-2697. (e) Caswell, D. S.; Spiro, T. G. *Inorg. Chem.* **1987**, *26*, 18-22.

(43) (a) Felix, F.; Ferguson, J.; Gudel, H. U.; Ludi, A. *Chem. Phys. Lett.* **1979**, *62*, 153-157. (b) Felix, F.; Ferguson, J.; Gudel, H. U.; Ludi, A. *J. Am. Chem. Soc.* **1980**, *102*, 4096-4102.



$\text{cm}^{-1}$ . This is almost twice as large as earlier estimates,<sup>34</sup> and is an independent measurement consistent with the electroabsorption result that the electronic interaction is greater in this complex than previously thought (see above). Furthermore, the observed transition energy can be used to calculate molecular orbital parameters and coefficients by using the model of Zwickel and Creutz.<sup>8,34,39</sup>  $\delta = 11\,000\text{ cm}^{-1}$ ,  $\beta = 8350\text{ cm}^{-1}$ ,  $c_M = 0.88$ , and  $c_L = 0.47$ .<sup>44</sup> Within the context of this model, the difference in the squares of the orbital coefficients corresponds to 55% of full charge transfer, which is closer to that measured from the electroabsorption experiment (32/f%) than a previous estimate (80%) based on indirect data.<sup>34</sup> Unfortunately, the low-energy feature in the electroabsorption spectrum of  $(\text{NH}_3)_5\text{Ru}(4,4'\text{-bpy})^{2+}$  is not sufficiently resolved from that of the main MLCT band to warrant a similar analysis, but roughly places the unresolved low-energy, nonbonding-to-antibonding transition somewhere between 15 000 and 17 000  $\text{cm}^{-1}$ .

$(\text{NH}_3)_5\text{Ru}(\text{pz})\text{H}^{3+}$  is the only complex to display a low-energy band that is well-resolved from the MLCT band. It has previously been assigned as due to a transition from a nonbonding ruthenium orbital to the ligand  $\pi^*$  orbital, thus preserving charge-transfer character even when significant delocalization due to back-bonding occurs.<sup>39</sup> While the line shape of the electroabsorption of this band is complex, the significant second-derivative contribution due to  $\Delta\mu$  strongly supports this interpretation.

**Biruthenium  $[(\text{NH}_3)_5\text{RuLRu}(\text{NH}_3)_5]^{4+}$  Complexes.** The biruthenium complexes all present complicated  $\Delta A(\nu)$  spectra in the visible region. The complexity is almost certainly due to the presence of multiple overlapping bands that may each have multiple types of derivatives contributing to the electroabsorption line shape. Spectral heterogeneity in these types of complexes may potentially arise if significant ion pairing or complex aggregation occurs, possibly with measurable electroabsorptive consequences. While ion pairing has been observed in similar types of complexes in low-dielectric media,<sup>66</sup> it seems likely that this phenomenon does not significantly contribute to the observed electroabsorption spectra of biruthenium complexes that are prepared at room temperature in relatively high-dielectric glycerol/water media and are then very rapidly frozen.

In the case of the  $[(\text{NH}_3)_5\text{Ru}]_2\text{L}^{4+}$  complexes, the presence of disproportionately large electroabsorptive effects corresponding to the low-energy, weakly absorbing wings of the absorption spectra is especially interesting. As in the monoruthenium complexes, these may nominally correspond to weakly allowed electronic transitions from nonbonding metal to antibonding ligand orbitals, which should occur at energies below that of the highly allowed MLCT transitions.<sup>36</sup> Since such transitions involve inherently weaker metal-ligand interactions, they may possess relatively larger  $|\Delta\mu|$  and may be more noticeably enhanced in an electric field. In this case, the separation between low- and high-energy electroabsorption effects is approximately equivalent to the stabilization energy due to metal-ligand back-bonding. These extra features may also be direct singlet-to-triplet MLCT transitions that gain intensity through spin-orbit coupling in a manner similar to that suggested for  $\text{Ru}(\text{bpy})_3^{2+}$ ,<sup>43</sup> which also exhibits a disproportionate electro-absorption in this spectral region.<sup>17</sup>

More speculatively, weak [2,2] to [1,3] intervalence absorptions may exist that could be sufficiently dipolar in weakly coupled complexes to appear as significant features in the electroabsorption spectrum. Roughly equal in energy to the sum of the ligand field splitting and the reorganization energy of charge transfer, this novel transition would formally correspond to the promotion of an electron from the  $t_{2g}$  orbitals of one ruthenium to the  $e_g$  orbitals of the other in octahedral ligand fields. Unlike a conventional MMCT absorptive transition, this should occur at relatively high energy in the visible to the near-ultraviolet region. Because such

an MMCT transition has been neither observed nor characterized previously in these systems, its energy relative to the primary MLCT band is unknown; on the basis of known values of the ligand field splitting in  $\text{Ru}(\text{NH}_3)_5(\text{H}_2\text{O})^{2+}$ , it may be more likely to contribute to deviations of  $\Delta A(\nu)$  from a sum of derivatives of the overall absorption at energies higher than 22 000  $\text{cm}^{-1}$ .<sup>45</sup> The convolution of highly dipolar effects from both the strongly allowed MLCT and nearby weak MMCT transitions remains as an intriguing possibility that awaits further experimental and theoretical support.

It is interesting to contrast these results for the (4+) complexes with an electroabsorption study of 1,4-bis[4'-(dimethylamino)-3',5'-dicyanophenyl]bicyclo[2.2.2]octane.<sup>12</sup> That study concluded that the lowest electronic absorptions arise from separate transitions localized on each half of the molecule; the excited-state dipole moments and polarizabilities are simply additive combinations of the dipoles and polarizabilities of the excited and unexcited halves of the molecule. This effect was modeled as arising from symmetry-breaking interactions with the solvent that predominate over interactions between the two halves. In contrast, both of the biruthenium (4+) complexes appear to behave very differently from their monoruthenium constituents and cannot simply be described as the limiting case of two localized charge transfers occurring within a larger molecular framework. The differences between these two types of complexes probably rest with the nature of the bridging ligand which, when conjugated as in pz or partially conjugated as in 4,4'-bpy, allows a larger electronic coupling than with bicyclooctane.

**Biruthenium  $[(\text{NH}_3)_5\text{RuLRu}(\text{NH}_3)_5]^{4+}$  Complexes.** As with the (4+) complexes, the electroabsorption effects for the visible absorption spectra of the mixed-valence complexes are difficult to interpret without independent information on the line shapes of overlapping transitions in this region. Qualitatively, however, the results are consistent with the picture of strong and weaker electronic couplings associated with the pyrazine and bipyridine ligands, respectively, which emerges from the other mono- and biruthenium complexes (see above). The complexities of the  $\Delta A$  spectra are understandable given the number of possible transitions in the visible region for these compounds, perhaps even including intervalence transitions between the  $t_{2g}$  orbitals on one metal and the  $e_g$  orbitals of the other, formally resulting in both charge transfer and a ligand field excited state on one metal. While this latter possibility has been suggested for mixed-valence complexes in principle,<sup>46-48</sup> few experiments to our knowledge have directly addressed it.<sup>49</sup> As discussed for the  $[(\text{NH}_3)_5\text{Ru}]_2\text{L}^{4+}$  complexes, while such transitions might be weak and masked in absorption, they nominally constitute significant charge transfers and might contribute appreciably to the electroabsorption line shape.

The near-infrared spectra of the mixed-valence complexes studied here, as well as others that followed,<sup>50,51</sup> have traditionally been interpreted by the simple yet elegant and powerful theory of Hush which, in the high-temperature and weak electronic coupling limits, relates the properties of an MMCT absorption band to parameters for thermal electron-transfer reactions.<sup>52</sup> The theory also permits the calculation of a delocalization parameter,

(45) Krentzien, H. Ph.D. Thesis, Stanford University, 1976.

(46) (a) Creutz, C. *Inorg. Chem.* **1978**, *17*, 3728-3725. (b) Lever, A. B. P. *Inorganic Electronic Spectroscopy*, 2nd ed.; Elsevier: Amsterdam, 1984; p 654.

(47) Hupp, J. T.; Meyer, T. J. *Inorg. Chem.* **1987**, *26*, 2332-2334.

(48) (a) Brunschwig, B. S.; Ehrenson, S.; Sutin, N. *J. Phys. Chem.* **1986**, *90*, 3657-3668. (b) Brunschwig, B. S.; Ehrenson, S.; Sutin, N. *J. Phys. Chem.* **1987**, *91*, 4714-4723.

(49) (a) A weak 25 000- $\text{cm}^{-1}$  band in Prussian blue has been assigned as  $t_{2g} \rightarrow e_g$  MMCT [Robin, M. B.; Day, P. *Adv. Inorg. Chem. Radiochem.* **1967**, *10*, 247-422]. (b) On a related note,  $t_{2g} \rightarrow e_g$  MMCT has been observed in the ion pair  $[\text{Co}(\text{NH}_3)_6]^{3+}/[\text{Ru}(\text{CN})_6]^{4-}$  [Vogler, A.; Kisslinger, J. *Angew. Chem.* **1982**, *94*, 64-65].

(50) (a) Powers, M. J.; Meyer, T. J. *J. Am. Chem. Soc.* **1980**, *102*, 1289-1297. (b) Callahan, R. W.; Keene, F. R.; Meyer, T. J.; Salmon, D. J. *J. Am. Chem. Soc.* **1977**, *99*, 1064-1073.

(51) Creutz, C. *Prog. Inorg. Chem.* **1983**, *30*, 1-73.

(52) (a) Hush, N. S. *Prog. Inorg. Chem.* **1967**, *8*, 391-444. (b) Hush, N. S. *Electrochim. Acta* **1968**, *13*, 1005-1023.

(44) High-energy MLCT transition energy  $\nu_h = (\delta^2 + 4\beta^2)^{1/2}$ ; low-energy MLCT transition energy  $\nu_l = (\delta + \nu_h)/2$ ;  $\delta = [L/H]L - [M/H]M$ ;  $\beta = [M/H]L$ ;  $E_\nu = \nu_h - \nu_l$ ;  $c_M$  and  $c_L$  are coefficients of pure metal and ligand orbitals, respectively, which comprise the molecular orbitals. See ref 34 for details.

$\xi$ , which describes the extent of mixing between states in which the unpaired electron completely resides on one metal or the other of the complex. The theory, while not appropriate for the pyrazine complex, has generally been regarded as providing a satisfactory model of the 4,4'-bipyridine complex.<sup>51</sup> Recently, however, even this success has been questioned.<sup>47</sup> Though many experimental and theoretical efforts have further augmented our understanding of the MMCT band in the mixed-valence complexes considered here,<sup>51,53,54</sup> it is remarkable that none has previously addressed or exploited the interesting effects of electric fields. Since the dipole moment of a molecule directly reflects its charge distribution, electroabsorption measurements can provide a general and convenient means of qualitatively assessing the degree of electronic delocalization in mixed-valence complexes; ideally, careful measurements of the changes in dipole moments upon charge transfer can provide quantitative information on electronic structures as well.

The low-energy portion of the near-infrared absorption band of  $[(\text{NH}_3)_5\text{Ru}]_2\text{pz}^{5+}$  decreases in intensity in an electric field, indicating an effect predominantly due to a perturbation of the transition dipole moment. The absence of an appreciable contribution by  $\Delta\mu$  to the observed  $\Delta A$  spectrum indicates that this transition involves little net movement of the centers of charge. This result directly demonstrates that the metal centers are so strongly coupled to each other that the unpaired electron is delocalized over both, even at 77 K; this description is consistent with a large body of indirect experimental evidence for this complex,<sup>51</sup> as well as theoretical analyses.<sup>53e,54</sup> The electroabsorption result does not support the prediction of sudden polarization contributing to charge-localized states in this molecule.<sup>55</sup> The small value of  $|\Delta\mu|$  needed to fit the  $\Delta A$  spectrum may well be due to some polarization in an inhomogeneous solvent environment. In principle, even a nominally symmetric molecule can show changes in dipole moment when placed in an asymmetric environment<sup>14,17,56</sup> due to polarization of the molecule by the solvent; sometimes this phenomenon can be surprisingly large for highly polarizable complexes placed in very asymmetric environments.<sup>56c</sup> By comparison, the near-infrared electroabsorption of  $[(\text{NH}_3)_5\text{Ru}]_2\text{pz}^{5+}$  in a reasonably polar solvent is not associated with large second- or first-derivative components, and hence the states associated with the near-IR transition appear to be neither polar nor highly polarizable.

The minor contribution by  $\Delta\mu$  to  $\Delta A(\nu)$  in the MMCT band when  $L = \text{pz}$  indicates that this complex is delocalized and possesses approximate electronic inversion symmetry. In such a case, the transition moment polarizability is also zero, and an estimate of the transition moment hyperpolarizability,  $B$ , is possible if it is assumed that only terms along the  $z$  axis (the metal-ligand-metal axis) are significant (see eq 1 and ref 23):

$$B = \frac{1}{2} S^{(1)} \cdot |\mathbf{M}|$$

By using the room temperature estimate<sup>2b</sup> of 0.03 for the oscillator strength of the near-infrared band and assuming it is also valid at 77 K, the electroabsorption results indicate that  $B$  is  $-8.7 \times 10^{-48} (\text{C}\cdot\text{m})/(\text{V}/\text{m})^2$ . This result suggests that an electric field of  $10^8 \text{ V}/\text{m}$  applied along the  $z$  axis would decrease the transition moment approximately 0.8%.

At energies higher than  $6500 \text{ cm}^{-1}$ , the near-infrared absorption and electroabsorption spectra of  $[(\text{NH}_3)_5\text{Ru}]_2\text{pz}^{5+}$  behave in a complicated manner. At 77 K, the absorption spectrum exhibits a slight shoulder on the high-energy side of the band, reflected in the heterogeneity of the electroabsorption. Variations across the near-infrared band have also been noted in MCD spectra at low temperatures.<sup>53b</sup> The unusual line shape in the near-infrared absorption of this molecule has been extensively modeled.<sup>53c,54</sup> The heterogeneity of effects in both MCD and electroabsorption experiments may reflect either (1) multiple electronic transitions arising from ruthenium orbitals that are not degenerate due to spin-orbit or lowered symmetry ligand field splittings,<sup>46a,47,48a</sup> or (2) vibronic bands<sup>54</sup> in the spectrum that possess differing susceptibilities to perturbing fields.

The electroabsorption spectrum of  $[(\text{NH}_3)_5\text{Ru}]_2\text{pz}^{5+}$  also possesses a very weak negative feature at  $\sim 12000 \text{ cm}^{-1}$ . A corresponding feature was also detected in the MCD spectrum<sup>53b</sup> and was speculatively assigned to be a singlet-to-triplet MLCT transition associated with the <sup>1</sup>MLCT transition at  $20000 \text{ cm}^{-1}$ . Within the context of simple molecular orbital models, a MLCT transition from essentially nonbonding metal orbitals to antibonding ligand orbitals may be an alternative assignment.<sup>36,57</sup> Another possibility is a localized d-d transition within the  $t_{2g}$  set.<sup>47</sup> In principle, since it corresponds to a local electronic excitation on a single ruthenium, this last possible type of transition should be distinguishable from the others since it will be associated with a much smaller  $\Delta\mu$  or  $\Delta\alpha$ . Thus, it is qualitatively consistent with the observed negative zeroth-derivative feature, though this experiment alone cannot definitively assign this transition in a delocalized complex.

A large  $\Delta\mu$  should accompany a true intervalence transition involving a large redistribution of electronic charge density from one metal center to the other. The near-infrared transition of  $[(\text{NH}_3)_5\text{Ru}]_2(4,4'\text{-bpy})^{5+}$  is such a case—the observed  $|\Delta\mu|$  of 28/fD indicates that the states involved are highly dipolar, and the unpaired electron is substantially localized. For the limiting case of full charge transfer over  $11.3 \text{ \AA}$  (the Ru-Ru distance),  $|\Delta\mu|$  will be 54 D. While very large, the experimentally measured value of  $|\Delta\mu|$  is still significantly smaller than this upper limit, suggesting a degree of electronic delocalization that is substantially larger than previous estimates based on the Hush theory, which concluded that the electron is  $>99.8\%$  localized on one metal center.<sup>32,58</sup> However, the use of this treatment to obtain quantitative information has recently been questioned for this and similar ruthenium complexes,<sup>47,48,59,60</sup> as well as a mixed-valence copper-containing protein.<sup>67</sup> As with the monoruthenium complexes, electrostatic interactions between the metal and ammine dipoles can alter the apparent  $|\Delta\mu|$ , though this effect should diminish in relative importance as the charge-transfer distance increases.<sup>27</sup> Other explanations consistent with some delocalization include inequivalent electronic couplings in the ground and excited phonon states, which could be tested if the ground state dipole moment is known.<sup>61,62</sup>

(53) (a) Best, S. P.; Clark, R. J. H.; McQueen, R. C. S.; Joss, S. J. *Am. Chem. Soc.* **1989**, *111*, 548–550. (b) Krausz, E.; Ludi, A. *Inorg. Chem.* **1985**, *24*, 939–943. (c) Furholz, U.; Joss, S.; Burgi, H.-B.; Ludi, A. *Inorg. Chem.* **1985**, *24*, 943–948. (d) Furholz, U.; Burgi, H.-B.; Wagner, F. E.; Stebler, A.; Ammeter, J. H.; Krausz, E.; Clark, R. J. H.; Stead, M. J.; Ludi, A. *J. Am. Chem. Soc.* **1984**, *106*, 121–123. (e) Brown, D. B. *Mixed Valence Compounds*; D. Reidel Publishing Co.: Dordrecht, Holland, 1980. (f) Beattie, J. K.; Hush, N. S.; Taylor, P. R.; Raston, C. L.; White, A. H. *J. Chem. Soc., Dalton Trans.* **1977**, 1121–1124. (g) Creutz, C. *Inorg. Chem.* **1978**, *17*, 3723–3725. (h) Hush, N. S. *Chem. Phys. Lett.* **1980**, *69*, 128–133. (i) Hammack, W. S.; Lowery, M. D.; Hendrickson, D. N.; Drickamer, H. G. *J. Phys. Chem.* **1988**, *92*, 1771–1774.

(54) (a) Piepho, S. B.; Krausz, E. R.; Schatz, P. N. *J. Am. Chem. Soc.* **1978**, *100*, 2996–3005. (b) Piepho, S. B. *J. Am. Chem. Soc.* **1988**, *110*, 6319–6326. (c) Piepho, S. B. *J. Am. Chem. Soc.* **1990**, *112*, 4179–4206. (d) Zhang, L.-T.; Ko, J.; Ondrechen, M. J. *J. Am. Chem. Soc.* **1987**, *109*, 1666–1671. (e) Ondrechen, M. J.; Ko, J.; Zhang, L.-T. *J. Am. Chem. Soc.* **1987**, *109*, 1672–1676. (f) Zhang, L.-T.; Ko, J.; Ondrechen, M. J. *J. Phys. Chem.* **1989**, *93*, 3030–3034.

(55) Chu, S.-Y.; Lee, S.-L. *Chem. Phys. Lett.* **1980**, *71*, 363–367.

(56) (a) Gerblinger, J.; Bogner, U.; Maier, M. *Chem. Phys. Lett.* **1987**, *141*, 31–35. (b) Kador, L.; Haarer, D.; Personov, R. *J. Chem. Phys.* **1987**, *86*, 5300–5307. (c) Gottfried, D. S.; Steffen, M. S.; Boxer, S. G. *Science* **1991**, *251*, 662–665.

(57) See footnote 30 in ref 39.

(58) We note, though, this is one of the largest  $|\Delta\mu|$  measured for any molecule. For example, an analogous organic donor-acceptor molecule, 4-amino-4'-nitrobiphenyl, in benzene possesses ground- and excited-state dipole moments of 6 and 22 D, respectively, and thus has  $|\Delta\mu| = 16 \text{ D}$ .<sup>10a</sup>

(59) Hupp, J. T.; Weaver, M. J. *J. Phys. Chem.* **1985**, *89*, 1601–1608.

(60) Interestingly, the complex  $[\text{Cl}(2,2'\text{-bpy})_2\text{Ru}]_2(4,4'\text{-bpy})^{3+}$  agrees extremely well with dielectric continuum models and may be a good candidate for further electroabsorption measurements (see ref 47).

(61) Meyer, T. J. In *Mechanistic Aspects of Inorganic Reactions*; Rorabacher, D. B.; Endicott, J. F., Eds.; American Chemical Society: Washington, DC, 1982.

Unfortunately, measurements of ground-state dipole moments of ionic species are very difficult to perform. Alternatively, less than a unit charge (in this case 0.54/*f*) may transfer due to significant but incomplete electronic delocalization across the bipyridyl bridge. The conformation of the 4,4'-bipyridine could play a key role in determining the degree of delocalization.<sup>40,42</sup> While the electroabsorption results for protonated and unprotonated (NH<sub>3</sub>)<sub>5</sub>Ru-(4,4'-bpy)<sup>2+</sup> are consistent with the idea that the bipyridyl conformation is unaffected by acidic interactions, they do suggest a conformation that permits some interaction between the two pyridyl rings. Finally, the centers of charge may be separated by less than 11.3 Å. The electroabsorption results suggest the minimum effective distance between the centers of charge would be 6/*f* Å, resulting from partial delocalization of the ruthenium charges onto the pyridyl rings. In principle, each of these possibilities may contribute to the difference between the observed and upper limit to  $\Delta\mu$ . Previous work has also shown that the solvent may significantly influence the degree of delocalization in mixed-valence complexes.<sup>63</sup> Electroabsorption experiments

(62) Differences in dipole moments and polarizabilities of the ground and excited vibrational states should be of great theoretical interest since they represent the mechanisms that confer intensity to infrared and Raman spectral lines, respectively. Moreover, such information might provide information on the dependence of electronic coupling on the vibrational levels of modes coupled to electron transfer, as well as indicate the relative ease with which solvent fluctuations can polarize the system. Application of the Stark effect to the infrared absorption of molecules adsorbed on metal surfaces has been discussed previously [Korzeniewski, C.; Shirts, R. B.; Pons, S. *J. Phys. Chem.* **1985**, *89*, 2297-2298].

(63) (a) Hupp, J. T.; Neyhart, G. A.; Meyer, T. J. *J. Am. Chem. Soc.* **1986**, *108*, 5349-5350. (b) Webb, R. J.; Geib, S. J.; Staley, D. L.; Rheingold, A. L.; Hendrickson, D. N. *J. Am. Chem. Soc.* **1990**, *112*, 5031-5042.

(64) Gress, M. E.; Creutz, C.; Quicksall, C. O. *Inorg. Chem.* **1981**, *20*, 1522-1528.

(65) Wishart, J. F.; Bino, A.; Taube, H. *Inorg. Chem.* **1986**, *25*, 3318-3321.

(66) Blackburn, R. L.; Hupp, J. T. *J. Phys. Chem.* **1990**, *94*, 1788-1793.

(67) Westmoreland, T. D.; Wilcox, D. E.; Baldwin, M. J.; Mims, W. B.; Solomon, E. I. *J. Am. Chem. Soc.* **1989**, *111*, 6106-6123.

(68) Trifluoromethanesulfonic (triflic) acid has also been used to form (NH<sub>3</sub>)<sub>5</sub>Ru(pz)H<sup>3+</sup>. The visible electroabsorption spectra of this complex yield electrooptic properties that do not significantly differ from those obtained when HCl is used to form the protonated ion. Since triflate is very different from chloride as a counterion, specific ion pairing effects are unlikely causes of the unusual line shape associated with the overall visible electroabsorption spectra of (NH<sub>3</sub>)<sub>5</sub>Ru(pz)H<sup>3+</sup>.

(69) The position of this near-infrared band associated with (NH<sub>3</sub>)<sub>5</sub>Ru-(pz)H<sup>3+</sup> does appear to depend on the counterion, shifting ~600 cm<sup>-1</sup> to higher energy when triflic acid is used as a source of protons. However, in each case, fits to the electroabsorption spectra indicate that a significant  $\Delta\mu$  exists.

as a function of solvent would be an interesting extension of the results obtained with glycerol/D<sub>2</sub>O. In any case, an internal consistency exists in the observation that the biruthenium complex bridged by bipyridine has a  $|\Delta\mu|$  which is roughly twice as large as in the monoruthenium complex.

## Summary

Electroabsorption spectra have been recorded for the optical charge-transfer spectra of (NH<sub>3</sub>)<sub>5</sub>RuL<sup>2+</sup> and [(NH<sub>3</sub>)<sub>5</sub>Ru]<sub>2</sub>L<sup>4+,5+</sup> where L is pyrazine or 4,4'-bipyridine. Analysis of the MLCT spectra of the monoruthenium complexes and of the near-infrared spectra of the binuclear mixed-valence complexes has yielded quantitative estimates of many of their molecular electric field interactive properties, including values for Tr $\Delta\alpha$  and  $|\Delta\mu|$ . In all cases, when the ligand is pyrazine, the values of  $|\Delta\mu|$  are small compared to the analogous bipyridyl complexes, indicating the much stronger metal-ligand interactions present with pyrazine. The protonated monoruthenium complexes are particularly remarkable in this regard. The extreme case of no significant  $|\Delta\mu|$  occurs in the pyrazine-bridged mixed-valence complex which directly demonstrates that it is electronically delocalized. Even where reliable quantitative analyses were not possible, a qualitative inspection of the electroabsorption spectra provides insight into the number and electrostatic nature of transitions that comprise the absorption spectra. Additionally, enhanced electroabsorptive features corresponding to weak absorptions appear in many of the spectra that have been discussed within previous molecular orbital models, yielding estimates of metal-ligand orbital mixing. Electroabsorption measurements of inorganic charge-transfer complexes should provide valuable information not only toward understanding their electronic structures and photophysical behavior in solution, but also for those interested in manipulating and exploiting their properties.

**Acknowledgment.** We are grateful to Professor Henry Taube in whose laboratory M.S. prepared the compounds used in this work. We are also very grateful to Professors Taube and Hush for their encouragement and insight, and to Professors Reimers and Hush for kindly sharing their theoretical work with us and stimulating our thoughts in this area. This work is supported by the donors of the Petroleum Research Fund, administered by the American Chemical Society, and by NSF Grant CHE-9002248; D.H.O. is a trainee of the Medical Scientist Training Program supported by Grant GM07365 from NIGMS.